



HAL
open science

Interdependence of plasma membrane nanoscale dynamics of a kinase and its cognate substrate underlies Arabidopsis response to viral infection

Marie-Dominique Jolivet, Anne-Flore Deroubaix, Marie Boudsocq, Nikolaj B Abel, Marion Rocher, Terezinha Robbe, Valérie Wattelet-Boyer, Jennifer Huard, Dorian Lefebvre, Yi-Ju Lu, et al.

► To cite this version:

Marie-Dominique Jolivet, Anne-Flore Deroubaix, Marie Boudsocq, Nikolaj B Abel, Marion Rocher, et al.. Interdependence of plasma membrane nanoscale dynamics of a kinase and its cognate substrate underlies Arabidopsis response to viral infection. *eLife*, 2024, 12, pp.RP90309. 10.7554/eLife.90309.2 . hal-04873172

HAL Id: hal-04873172

<https://hal.science/hal-04873172v1>

Submitted on 8 Jan 2025

HAL is a multi-disciplinary open access archive for the deposit and dissemination of scientific research documents, whether they are published or not. The documents may come from teaching and research institutions in France or abroad, or from public or private research centers.

L'archive ouverte pluridisciplinaire **HAL**, est destinée au dépôt et à la diffusion de documents scientifiques de niveau recherche, publiés ou non, émanant des établissements d'enseignement et de recherche français ou étrangers, des laboratoires publics ou privés.



Distributed under a Creative Commons Attribution 4.0 International License

Interdependence of plasma membrane nanoscale dynamics of a kinase and its cognate substrate underlies *Arabidopsis* response to viral infection


Reviewed Preprint

v2 • October 18, 2024

Revised by authors

Reviewed Preprint

v1 • September 14, 2023

Marie-Dominique Jolivet, Anne-Flore Deroubaix, Marie Boudsocq, Nikolaj B Abel, Marion Rocher, Terezinha Robbe, Valérie Wattelet-Boyer, Jennifer Huard, Dorian Lefebvre, Yi-Ju Lu, Brad Day, Grégoire Saias, Jahed Ahmed, Valérie Cotelle, Nathalie Giovinazzo, Jean-Luc Gallois, Yasuyuki Yamaji, Sylvie German-Retana, Julien Gronnier, Thomas Ott, Sébastien Mongrand, Véronique Germain 

Univ. Bordeaux, CNRS, Laboratoire de Biogenèse Membranaire (LBM), UMR 5200, Villenave d'Ornon, France • Université Paris-Saclay, CNRS, INRAE, Univ Evry, Université Paris Cité, Institute of Plant Sciences Paris-Saclay (IP52), Gif-sur-Yvette, France • Faculty of Biology, University of Freiburg, Freiburg, Germany • Faculty of Biology, University of Munich (LMU), Planegg-Martinsried, Germany • Department of Plant, Soil and Microbial Sciences, Michigan State University, East Lansing, USA • Laboratoire de Recherche en Sciences Végétales (LRSV), Université de Toulouse, CNRS, UPS, Toulouse INP, Auzeville-Tolosane, France • INRAE, GAFL, Montfavet, France • Graduate School of Agricultural and Life Sciences, The University of Tokyo, Bunkyo-ku, Japan • UMR 1332 BFP, INRAE Univ. Bordeaux, Villenave d'Ornon, France • Center of Plant Molecular Biology (ZMBP), University of Tübingen, Tübingen, Germany • CIBSS – Centre for Integrative Biological Signalling Studies, University of Freiburg, Freiburg, Germany

 https://en.wikipedia.org/wiki/Open_access

 Copyright information

Abstract

Plant viruses represent a risk to agricultural production and as only a few treatments exist, it is urgent to identify resistance mechanisms and factors. In plant immunity, plasma membrane (PM)-localized proteins play an essential role in sensing the extracellular threat presented by bacteria, fungi or herbivores. Viruses are intracellular pathogens and as such the role of the plant PM in detection and resistance against viruses is often overlooked. We investigated the role of the partially PM-bound Calcium-dependent protein kinase 3 (CPK3) in viral infection and we discovered that it displayed a specific ability to hamper viral propagation over CPK isoforms that are involved in immune response to extracellular pathogens. More and more evidence support that the lateral organization of PM proteins and lipids underlies signal transduction in plants. We showed here that CPK3 diffusion in the PM is reduced upon activation as well as upon viral infection and that such immobilization depended on its substrate, Remorin (REM1.2), a scaffold protein. Furthermore, we discovered that the viral infection induced a CPK3-dependent increase of REM1.2 PM diffusion. Such interdependence was also observable regarding viral propagation. This study unveils a complex relationship between a kinase and its substrate that contrasts with the commonly described co-stabilisation upon activation while it proposes a PM-based mechanism involved in decreased sensitivity to viral infection in plants.

eLife Assessment

The study is considered **important** with **solid** evidence that demonstrates the impact of plasma membrane nano-domains and protein interactions in the plant defence response to viruses. It includes a molecular understanding of the role of a calcium dependent kinase (CPK3) and a remorin protein in the cell-to-cell spread of viruses and cytoskeletal dynamics demonstrating, conclusively, the role of CPK3 with multiple lines of evidence. The work opens avenues to investigate different viruses and other plasma membrane proteins to gain a fuller picture of the involvement of plasmodesmata and other nanodomains in virus spreading.

<https://doi.org/10.7554/eLife.90309.2.sa3>

Introduction

Viruses are intracellular pathogens, carrying minimal biological material and strictly relying on their host for replication and propagation. They represent a critical threat to both human health and food security. In particular, potexvirus epidemics like the one caused by pepino mosaic virus dramatically affect crop production¹ and the lack of chemical treatments available makes it crucial to develop inventive protective methods. Unlike their animal counterparts, which enter host cells by interacting directly with the plasma membrane (PM), plant viruses have to rely either on mechanical wounding or insect vectors to cross the plant cell wall¹. For this reason, only a few PM-localized proteins were identified as taking part in immunity against viruses^{2,3}. Among them, members of the REMORIN (REM) protein family were shown to be involved in viral propagation, with varying mechanisms depending on the studied viral genera⁴⁻⁹. REM proteins are well-known for their heterogeneous distribution at the PM, forming nanodomains (ND), PM nanoscale environments that display a composition different from the surrounding PM^{10,11}. Increasing evidence supports the role of ND in signal transduction, with the underlying idea that the local accumulation of proteins allows amplification and specification of the signal¹¹. For example, *Arabidopsis* RHO-OF-PLANT 6 accumulates in distinct ND upon osmotic stress and auxin treatment in a dose-dependent way for the latter¹². Recently, *Arabidopsis* REM1.2 (later named REM1.2) was demonstrated to form clusters upon exposure to the bacterial effector flg22 to support the condensation of *Arabidopsis* FORMIN 6 and to induce actin cytoskeleton remodeling¹³. However, unlike the canonical mechanism describing the accumulation of proteins in ND upon stimulation¹²⁻¹⁴, we showed previously that *Solanum tuberosum* REM1.3 (StREM1.3) ND were disrupted and the diffusion of individual proteins increased in response to a viral infection¹⁵. StREM1.3 lateral organization in lipid bilayers was also shown to be modified upon its phosphorylation status, both *in vitro* and *in vivo*^{15,16}. The role of such protein dispersion upon stimuli is not understood yet and only a few similar cases are reported in the literature^{17,18}. REM1.2 was identified as a substrate of the partially membrane-bound CALCIUM-DEPENDENT PROTEIN KINASE 3 (CPK3)¹⁹. CPK3 is involved in defense response against herbivores, bacteria and viruses and was recently proposed to be at cross-roads between pattern-triggered immunity and effector-triggered immunity^{15,20,21}. We showed previously that transient over-expression of CPK3 in *N. benthamiana* was able to hamper potato virus X (PVX, potexvirus) cell-to-cell propagation¹⁵. Although partially PM localized, the role of CPK3 PM localization in immunity was never investigated for any pathogen. As the PVX cannot infect *Arabidopsis thaliana*, the dedicated plant model for genetic studies, we used an alternative virus model able to infect this species, the plantago asiatica mosaic virus (PIAMV)^{22,23} to investigate the role of CPK3 and of its PM localization in potexvirus propagation. We were able to highlight the specific role of CPK3 among other immune-related

CPKs^{24,26} in this context. Also, we demonstrated that CPK3 membrane localization was required to hamper viral cell-to-cell propagation and, using single-particle tracking photoactivated light microscopy (spt-PALM), we discovered that CPK3 diffusion was reduced upon activation and viral infection. Interestingly, this reduction of PM diffusion depended on the expression of Group 1 REM while viral-induced REM1.2 increased PM diffusion depended on CPK3. Overall, our data allowed us to propose a model for a PM-localized mechanism involved in the reduction of potexvirus propagation, which will encourage further exploration of the involvement of the PM in viral immunity.

Results

Arabidopsis thaliana calcium-dependent protein kinase 3 (CPK3) specifically restricts PIAMV propagation

We previously showed that transient overexpression of *Arabidopsis* CPK3 in *N. benthamiana* leaves restricted the propagation of the potexvirus potato virus X (PVX)¹⁵. CPKs are encoded by a large gene family of 34 members in *Arabidopsis*²⁷. To evaluate the functional redundancy between CPKs regarding viral propagation, a series of *Arabidopsis* lines mutated for CPK1, CPK2, CPK3, CPK5, CPK6 or CPK11, that are involved in plant resistance to various pathogens^{21,24,26,28}, were analyzed in a viral propagation assay. Because PVX does not infect *Arabidopsis*, we used instead a binary plasmid encoding for the genomic structure of a GFP-tagged PIAMV^{22,23}, a potexvirus that is capable of infecting a wide range of plant hosts, including *Arabidopsis*. Agrobacterium carrying PIAMV-GFP were infiltrated in *A. thaliana* leaves and GFP-fluorescent infection foci were observed 5 days post infiltration (dpi) (Figure 1 – figure supplement 1). The following combinations of mutants were tested: the *cpk1 cpk2* double mutant²⁵, the *cpk5 cpk6* double mutant²⁴, the triple mutant *cpk5 cpk6 cpk11*²⁴ and the two quadruple mutants *cpk1 cpk2 cpk5 cpk6*²⁵ and *cpk3 cpk5 cpk6 cpk11*²⁶. No significant difference of PIAMV-GFP infection foci area was detected between Col-0, *cpk1 cpk2*, *cpk5 cpk6*, *cpk1 cpk2 cpk5 cpk6* and *cpk5 cpk6 cpk11*, demonstrating that CPK1, CPK2, CPK5, CPK6 and CPK11 are not involved in PIAMV propagation (Figure 1A, 1B). However, a 20 % increase of PIAMV-GFP infected area was observed in *cpk3 cpk5 cpk6 cpk11* quadruple mutant relative to the control Col-0, which indicates that CPK3 could play a specific role in viral propagation. Since group 1 REMs are known substrates of CPK3¹⁹, we checked REM1.2 phosphorylation specificity by the CPK isoforms tested in viral propagation (Figure 1 – figure supplement 2). CPK1, 2 and 3 displayed the strongest kinase activity on REM1.2 while CPK5, CPK6 and CPK11 displayed a residual activity. In contrast, all 6 CPKs phosphorylated the generic substrate histone, suggesting some substrate specificity for REM1.2 *in vitro*. Since CPK1 and CPK2 were described to be mainly localized within the peroxisome²⁹ and endoplasmic reticulum³⁰, respectively, we hypothesize that they likely do not interact *in vivo* with PM-localized REM1.2³¹.

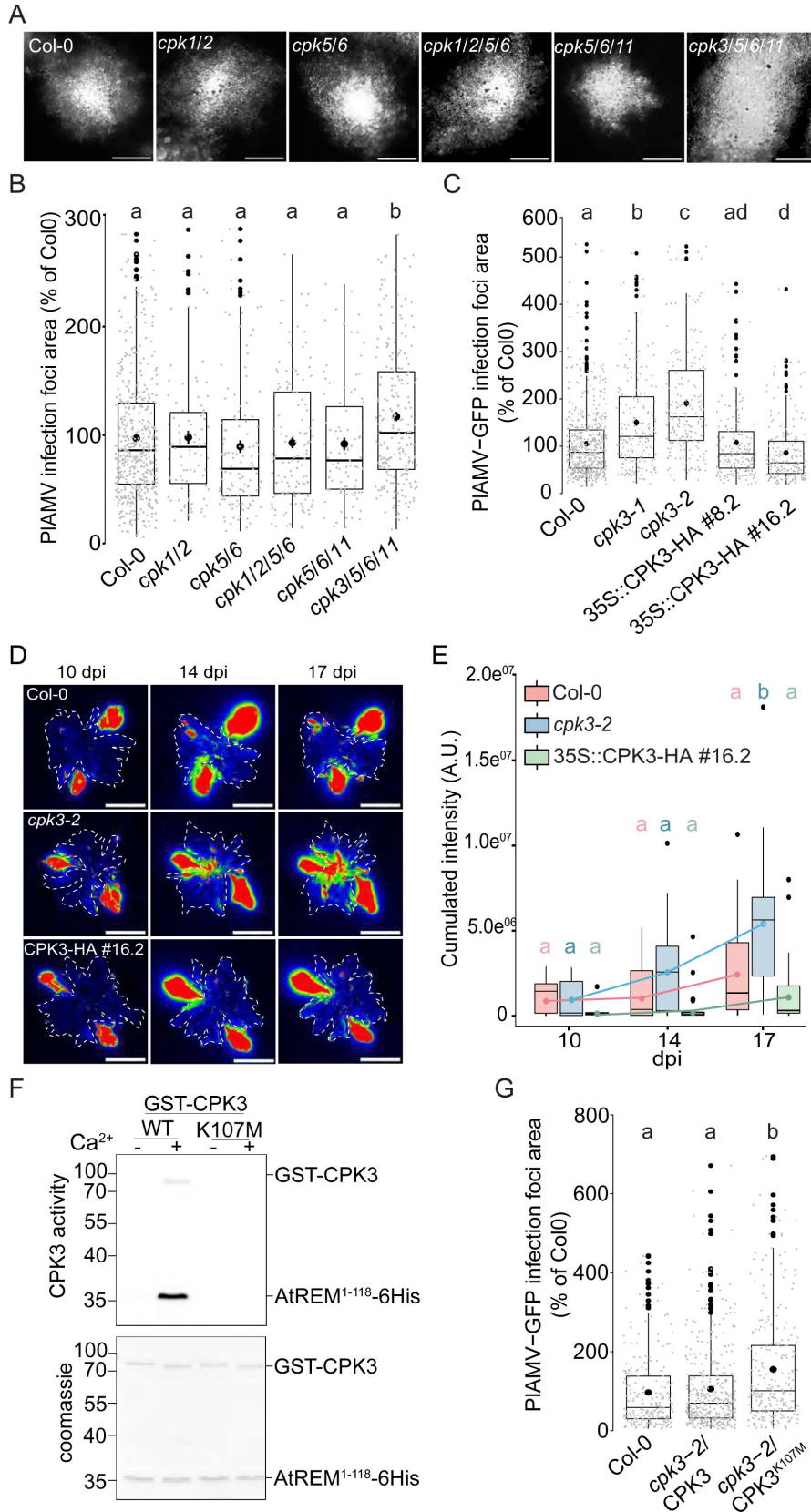


Figure 1.

***Arabidopsis thaliana* calcium-dependent protein kinase 3 (CPK3) is specifically involved in the restriction of PIAMV cell-to-cell movement.**

A. Representative images of PIAMV-GFP infection foci at 5 dpi in the different mutant backgrounds. Scale bar = 500 μm

B. Box plots of the mean area of PIAMV-GFP infection foci 5 days after infection in CPK multiple mutant lines, normalized to the mean area measured in Col-0. Three independent biological repeats were performed, with at least 47 foci per experiment and per genotype. Significant differences were revealed using a One-Way ANOVA followed by a Tukey's multiple comparison test. Letters are used to discriminate between statistically different conditions ($p < 0.05$).

C. Box plots of the mean area of PIAMV-GFP infection foci in *cpk3-1* and *cpk3-2* single mutants and in CPK3 over-expressing lines (Pro35S:CPK3-HA #8.2 and Pro35S:CPK3-HA #16.2), normalized to the mean area measured in Col-0. Three independent biological repeats were performed, with at least 56 foci per experiment and per genotype. Significant differences were revealed using a One-Way ANOVA followed by a Tukey's multiple comparison test. Letters are used to discriminate between statistically different conditions ($p < 0.05$).

D. Representative images of *A. thaliana* plants infected with PIAMV-GFP and imaged with a CCD Camera from 10 to 17 dpi. The region of interest used for measurement of pixel intensity is circled with a white dotted line. Multicolored scale is used to enhance contrast and ranges from blue (low intensity) to red (high intensity). Scale bar = 4 cm.

E. Box plots of the mean cumulated intensity measured in infected leaves in Col-0, *cpk3-2* and Pro35S:CPK3-HA #16.2 during systemic viral propagation. Two independent experiments were conducted. Statistical differences could be observed between the genotypes and time-points using a Kruskal-Wallis followed by a Dunn's multiple comparison test ($p < 0.05$). For clarity, only the results of the statistical test of the comparison of the different time-points (10, 14 and 17 dpi) within a genotype are displayed and are color-coded depending on the genotype.

F. Kinase activity of CPK3 dead variant. Recombinant proteins GST-CPK3 WT and K107M were incubated with REM1.2¹⁻¹¹⁸-6His in kinase reaction buffer in the presence of EGTA (-) or 100 μM free Ca^{2+} (+). Radioactivity is detected on dried gel (upper panel). The protein amount is monitored by Coomassie staining (lower panel).

G. Box plots of the mean area of PIAMV-GFP infection foci in *cpk3-2* complemented lines *cpk3-2/Pro35S:CPK3-myc* and *cpk3-2/Pro35S:CPK3^{K107M}-myc*. Three independent biological repeats were performed, with at least 51 foci per experiment and per genotype. Significant differences were revealed using a One-Way ANOVA followed by a Tukey's multiple comparison test. Letters are used to discriminate between statistically different conditions ($p < 0.0001$).

To further confirm a role for CPK3 in PIAMV infection, two independent knock-out (KO) lines for CPK3, *cpk3-1*³² and *cpk3-2*¹⁹ along with two independent lines overexpressing CPK3 (i.e., Pro35S:CPK3-HA-OE #8.2 and Pro35S:CPK3-HA-OE#16.2⁷²) (Figure 1 – figure supplement 3) were infiltrated with PIAMV-GFP. In both *cpk3-1* and *cpk3-2* KO lines, PIAMV-GFP propagation was significantly enhanced (40 to 60% compared with WT Col-0), whereas the over-expression lines Pro35S:CPK3-HA-OE#8.2 and Pro35S:CPK3-HA-OE#16.2⁷² showed 10% and 20 % restriction of the foci area, respectively (Figure 1C). To assess whether CPK3 regulates viral propagation at the plant level, the propagation of PIAMV-GFP in systemic leaves was assessed in 3-week-old *cpk3-2* and Pro35S:CPK3-HA-OE#16.2 lines along with Col-0 at 10, 14 and 17 days post infection (dpi) using a CCD Camera equipped with a GFP filter (Figure 1 – figure supplement 1). We observed that loss of CPK3 led to an increase of PIAMV-GFP propagation in distal leaves during the course of our assay

while the overexpression of CPK3 did not hamper PLAMV-GFP to a greater extent than WT Col-0 (**Figure 1D** [↗](#) and **E** [↗](#)). This would suggest that CPK3 effect on PLAMV propagation is predominant at the site of infection. For this reason, we concentrated on foci in local leaves for further study.

CPK3 Lysine 107 functions as an ATP binding site and its substitution into methionine abolishes CPK3 activity *in vitro*²¹ [↗](#). In good agreement, we observed that CPK3^{K107M} can no longer phosphorylate REM1.2 *in vitro* (**Figure 1F** [↗](#)). To test whether CPK3 kinase activity is required for its function during PLAMV infection, we analyzed the propagation of PLAMV-GFP in complementation lines of *cpk3-2* with WT CPK3 or with CPK3^{K107M}. While the WT CPK3 fully complemented *cpk3-2* mutant, it was not the case with *cpk3-2/Pro35S:CPK3^{K107M}*, which displayed larger infection foci area compared to WT Col-0 (**Figure 1G** [↗](#)).

Taken together, these results demonstrate a specific involvement for CPK3 among other previously described immune-related CPKs in limiting PLAMV infection.

PLAMV infection induces a decrease in CPK3 PM diffusion

We next wondered whether CPK3 accumulation is regulated at transcriptional and translational level upon PLAMV infection. RT-qPCR and western blots of CPK3 in Col-0 showed that both transcript and protein levels remained unchanged during PLAMV infection (Figure 2 – figure supplement 1). CPK3 is partially localized within the PM and is myristoylated at Glycine 2, a modification required for its association with membranes¹⁹ [↗](#). To test whether CPK3 membrane localization is required to hamper PLAMV propagation, we transformed *cpk3-2* mutant with either ProUbi10:CPK3-mRFP1.2 or ProUbi10:CPK3^{G2A}-mRFP1.2 (**Figure 2A** [↗](#)) and tested PLAMV infection. We observed that, in contrary to ProUbi10:CPK3-mRFP1.2, ProUbi10:CPK3^{G2A}-mRFP1.2 did not complement *cpk3-2* (**Figure 2B** [↗](#)). These observations indicate that CPK3 association with the PM is required for its function in inhibiting PLAMV propagation. We next analyzed the organization of CPK3 PM pool in absence or presence of PLAMV-GFP using confocal microscopy. Imaging of the surface of *A. thaliana* leaf epidermal cells expressing *CPK3-mRFP1.2* showed that the protein displayed a heterogeneous pattern at the PM in both conditions (**Figure 2C** [↗](#)), although the limitation in lateral resolution of confocal microscopy hindered a more detailed analysis of CPK3 PM organization.

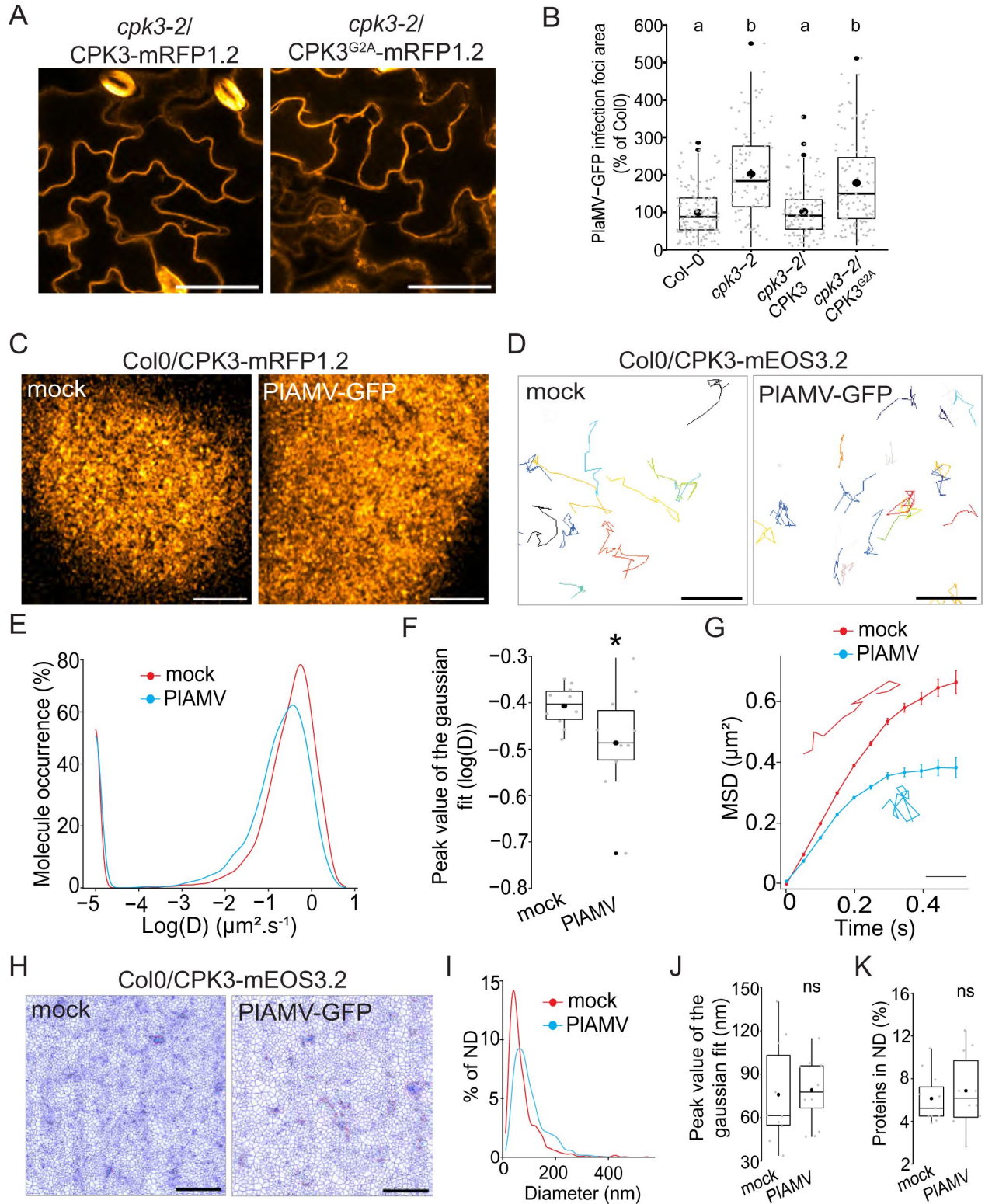


Figure 2.

CPK3 diffusion decreases upon PIAMV infection in *Arabidopsis thaliana*

A. Confocal images of the secant view of *A. thaliana* epidermal cells of the *cpk3-2*/CPK3-mRFP1.2 or *cpk3-2*/ProUbi10:CPK3^{G2A}-mRFP1.2. Scale bar = 5 μm

B. Box plots of the mean area of PIAMV-GFP infection foci in *cpk3-2* and complemented lines *cpk3-2*/ProUbi10:CPK3-mRFP1.2 and *cpk3-2*/ProUbi10:CPK3^{G2A}-mRFP1.2. Three independent biological repeats were performed, with at least 32 foci per experiment and per genotype. Significant differences were revealed using a One-Way ANOVA followed by a Tukey's multiple comparison test. Letters are used to discriminate between statistically different conditions ($p < 0.0001$).

C. Confocal images of the surface view of *A. thaliana* epidermal cells of the Col-0/ProUbi10:CPK3-mRFP1.2, infiltrated either with free GFP ("mock") or PIAMV-GFP. Scale bar = 5 μm

D. Representative trajectories of Col-0/CPK3-mEOS3.2 infiltrated either with free GFP ("mock") or PIAMV-GFP; Scale bar = 2 μm

E. Distribution of the diffusion coefficient (D), represented as log(D) for Col-0/ProUbi10:CPK3-mEOS3.2 five days after infiltration with free GFP ("mock") or PIAMV-GFP. Data were acquired from at least 8086 trajectories obtained in at least 16 cells over the course of three independent experiments.

F. Box plot of the mean peak value extracted from the Gaussian fit of log(D) distribution. Significant difference was revealed using a Mann-Whitney test. *: $p < 0.05$.

G. Mean square displacement (MSD) over time of Col-0/ProUbi10:CPK3-mEOS3.2 five days after infiltration with free GFP ("mock") or PIAMV-GFP. Representative trajectories extracted from [Figure 2D](#) illustrate each curve. Scale bar = 1 μm. Data were acquired from at least 16 cells over the course of three independent experiments.

H. Voronoi tessellation illustration of Col-0/ProUbi10:CPK3-mEOS3.2 five days after infiltration with free GFP ("mock") or PIAMV-GFP. ND are circled in red. Scale bar = 2 μm

I. Distribution of the ND diameter of Col-0/ProUbi10:CPK3-mEOS3.2 five days after infiltration with free GFP ("mock") or PIAMV-GFP.

J. Box plot representing the mean peak value of ND diameter extracted from the Gaussian fit of [Figure 2I](#). No significant differences were revealed using a Mann-Whitney test.

K. Boxplot of the proportion of Col-0/ProUbi10:CPK3-mEOS3.2 detections found in ND five days after infiltration with free GFP ("mock") or PIAMV-GFP. No significant differences were revealed using a Mann-Whitney test.

Thus, we used single particle tracking phospho-activated localization microscopy (sptPALM) which overcomes the diffraction limit of confocal microscopy and allows the analysis of the diffusion and organization of single molecules. We used a translational fusion of CPK3 with the true monomeric photoconvertible fluorescent protein mEOS3.2³³ expressed in stable transgenic *Arabidopsis* lines. We imaged these materials in control and upon PIAMV infection. We tracked single molecule trajectories ([Figure 2D](#)) from which CPK3 diffusion coefficient (D) was calculated. We observed that CPK3 proteins were overall mobile in control and infected conditions ($\log(D) > -2$; [Figure 2E](#)) although CPK3 diffusion was reduced upon PIAMV infection ([Figure 2F](#)). Analysis of the mean squared displacement (MSD), describing the surface explored by single molecules overtime, showed that CPK3 displayed a more confined behavior during a PIAMV infection than in healthy

conditions (**Figure 2G** [↗](#)). Additionally, we performed cluster analysis using Voronoï tessellation, a computation method that segments super-resolution images into polygons based on the local molecule density³⁴ [↗](#). Voronoï analysis showed that no difference occurred in CPK3 cluster size or proportion of protein localized in cluster upon viral infection (**Figure 2H-K** [↗](#)). Taken together, these results show that CPK3 diffusion parameters were modified upon PIAMV infection, although the nano-organization of the proteins was maintained.

Truncation of CPK3 auto-inhibitory domain induces its confinement and accumulation in PM ND

CPK3 bears an auto-inhibitory domain that folds over the kinase domain and inhibits its kinase activity in the absence of calcium³⁵ [↗](#),³⁶ [↗](#). The truncation of this domain along with the C-terminal regulatory domain results in a calcium-independent, constitutively active CPK3 (CPK3^{CA})²⁴ [↗](#) that is lethal when stably expressed in *Arabidopsis*³⁷ [↗](#). For this reason, CPK3^{CA} was transiently expressed in *N. benthamiana* for further analysis. We observed that although both ProUbi10:CPK3-mRFP1.2 and ProUbi10:CPK3^{CA}-mRFP1.2 were partially cytosolic when transiently expressed in *N. benthamiana* (Figure 3 – figure supplement 1), ProUbi10:CPK3^{CA}-mRFP1.2 displayed a PM organization in domains discernable by confocal microscopy (**Figure 3A** [↗](#)).

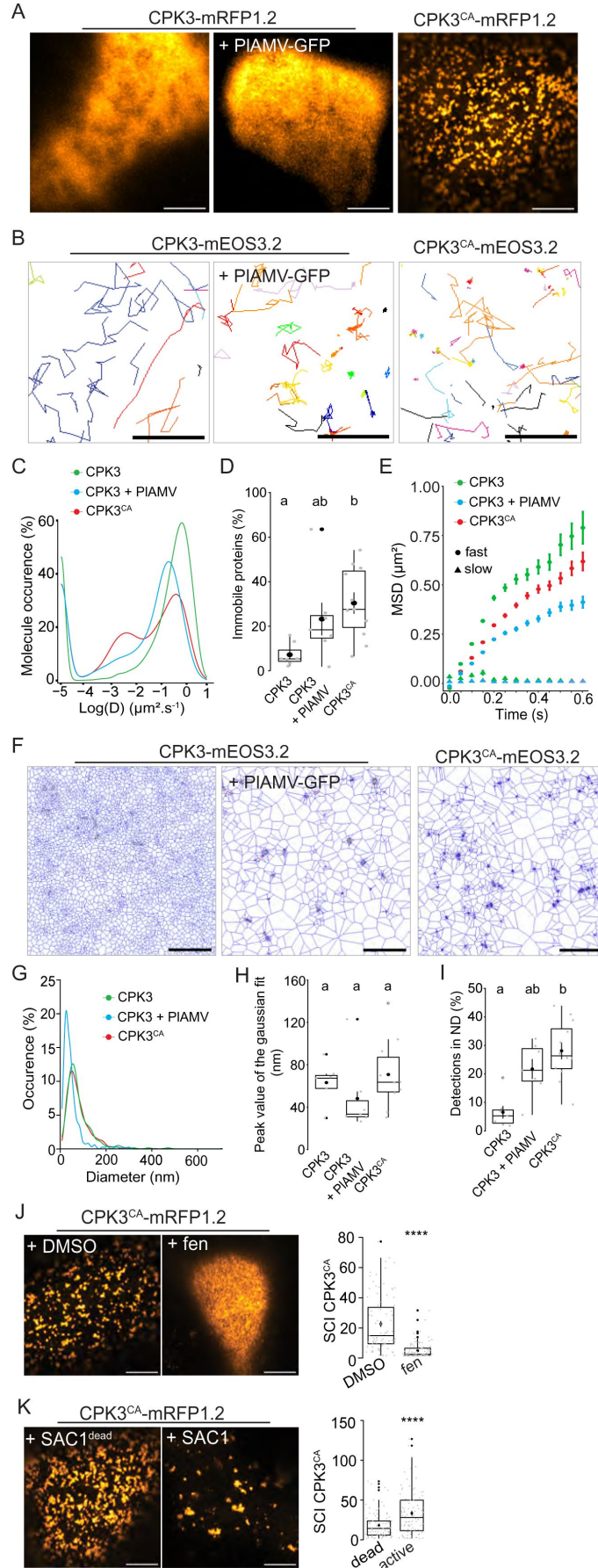


Figure 3.

PIAMV-induced activation of CPK3 in *N. benthamiana* induces its confinement and clustering in PM domains

- A. Confocal images of the surface view of *N. benthamiana* epidermal cells transiently expressing ProUbi10:CPK3-mRFP1.2, ProUbi10:CPK3-mRFP1.2 + PIAMV-GFP or ProUbi10:CPK3^{CA}-mRFP1.2. Scale bar = 5µm
- B. Representative trajectories of ProUbi10:CPK3-mEOS3.2, ProUbi10:CPK3.2-mEOS3.2 + PIAMV and ProUbi10:CPK3^{CA}-mEOS3.2. Scale bar = 2µm.
- C. Distribution of the diffusion coefficient (D), represented as log(D) for ProUbi10:CPK3-mEOS3.2, ProUbi10:CPK3-mEOS3.2 + PIAMV-GFP and ProUbi10:CPK3^{CA}-mEOS3.2. Data were acquired from at least 6144 trajectories obtained in at least 15 cells over the course of three independent experiments.
- D. Box plots of the fraction of immobile proteins (log(D)<-2). Significant differences were revealed using a One-Way ANOVA followed by a Tukey's multiple comparison test. Letters are used to discriminate between statistically different conditions (p<0.005).
- E. Mean square displacement (MSD) over time of fast (circle) or slow (triangle) diffusing ProUbi10:CPK3-mEOS3.2, ProUbi10:CPK3-mEOS3.2 + PIAMV-GFP, ProUbi10:CPK3^{CA}-mEOS3.2. Standard error is displayed from three independent experiments.
- F. Voronoi tessellation illustration of ProUbi10:CPK3-mEOS3.2, ProUbi10:CPK3-mEOS3.2 + PIAMV-GFP and ProUbi10:CPK3^{CA}-mEOS3.2. ND are circled in red. Scale bar = 2µm
- G. Distribution of the ND diameter of ProUbi10:CPK3-mEOS3.2, ProUbi10:CPK3-mEOS3.2 + PIAMV-GFP and ProUbi10:CPK3^{CA}-mEOS3.2
- H. Box plot representing the mean peak value of ND diameter extracted from the Gaussian fit of **Figure 3G**. No significant differences were revealed using a Kruskal-Wallis followed by a Dunn's multiple comparison test.
- I. Boxplot of the proportion of detections found in ND of ProUbi10:CPK3-mEOS3.2, ProUbi10:CPK3-mEOS3.2 + PIAMV-GFP and ProUbi10:CPK3^{CA}-mEOS3.2. Significant differences were revealed using a Kruskal-Wallis followed by a Dunn's multiple comparison test. Letters are used to discriminate between statistically different conditions (p<0.005).
- J. Left: Confocal images of the surface view of *N. benthamiana* epidermal cells transiently expressing ProUbi10:CPK3^{CA}-mRFP1.2 and infiltrated with either DMSO or 50 µg/mL fenpropimorph. Scale bar = 5µm; Right: Box plot of the mean Spatial Clustering Index (SCI) of CPK3^{CA}. At least three experiments were performed, with at least 10 cells per experiment; statistical significance was determined using a Student *t*-test, ****: p < 0.0001.
- K. Left: Confocal images of the surface view of *N. benthamiana* epidermal cells transiently co-expressing ProUbi10:CPK3^{CA}-mRFP1.2 with active or dead SAC1, mutated for its phosphatase activity. Scale bar = 5µm; Right: Box plot of the mean SCI of CPK3^{CA}. At least three experiments were performed, with at least 10 cells per experiment; statistical significance was determined using a Student *t*-test, ****: p < 0.0001.

We analyzed the dynamics of ProUbi10:CPK3-mEOS3.2 and ProUbi10:CPK3^{CA}-mEOS3.2 by spt-PALM (**Figure 3B**). We observed that the fraction of immobile ProUbi10:CPK3^{CA}-mEOS3.2 molecules (log(D) < -2) is more abundant than for ProUbi10:CPK3-mEOS3.2 in absence of viral infection while no significant difference could be deciphered upon PIAMV infection (**Figure 3C** and **D**). In addition, MSD analysis showed that the motion of CPK3-mEOS3.2 mobile fraction is

less confined than the one of CPK3^{CA}-mEOS3.2 and CPK3-mEOS3.2 upon PLAMV infection (**Figure 3E**). Overall, this indicates that the mobile and immobile fraction of CPK3 is affected upon PLAMV infection and upon truncation of its auto-inhibitory domain, respectively.

Cluster analysis of CPK3 was performed using tessellation on the localization data obtained with spt-PALM (**Figure 3F**). Although we did not observe any significant differences in distribution of cluster sizes between all compared conditions (**Figure 3G** and **H**), CPK3^{CA} displayed a significantly higher proportion of proteins localized in ND compared to CPK3 (**Figure 3I**).

While the mechanism(s) governing the clustering of membrane proteins are not fully described, it is widely accepted that lateral organization involves – to some extent – protein-lipid interactions and lipid-lipid organization^{10,11,38}. We observed that the integrity of ProUbi10:CPK3^{CA}-mRFP1.2 organization relied on sterols and phosphoinositides. Indeed, treatment with fenpropimorph, a well-described inhibitor of sterol biosynthesis³⁹, abolished CPK3^{CA} ND organization (**Figure 3J**), and the co-expression of ProUbi10:CPK3^{CA}-mRFP1.2 with the yeast phosphatidylinositol-4-phosphate (PI4P)-specific phosphatase SAC1 targeted to the PM⁴⁰, led to sparser and bigger domains (**Figure 3K**), which suggested that PI4P is not required for CPK3^{CA} ND formation but for its regulation.

All together these observations show that either removal of the auto-inhibitory domain or infection with PLAMV-GFP modifies CPK3 dynamics within the PM ; a mechanism which could be at stake for kinase activation.

PLAMV infection induces an increase in REM1.2 PM diffusion

Group 1 REMs are one of the targets of CPK3 and we previously demonstrated that the restriction of PVX propagation by CPK3 overexpression depended on endogenous group 1 NbREMs¹⁵. Four REM isoforms belong to the group 1 in *Arabidopsis*: REM1.1, REM1.2, REM1.3 and REM1.4⁴¹. *REM1.2* and *REM1.3* are amongst the 10% most abundant transcripts in *Arabidopsis* leaves while REM1.1 was not detected in recently published leaf transcriptomes and proteomes⁴². Therefore, we focused on the three isoforms REM1.2, REM1.3 and REM1.4. REMs are described as scaffold proteins⁴³, for which physiological function depends on the proteins they interact with and their phosphorylation status⁴⁴. As recently described in⁴⁵, REM1.2 and REM1.3 share 95% of their interactome, suggesting that they are functionally redundant. To address this, we isolated single T-DNA mutants *rem1.2*, *rem1.3* and *rem1.4* (SALK_117637.50.50.x, SALK_117448.53.95.x and SALK_073841.47.35, respectively) and crossed them to obtain the double mutant *rem1.2 rem1.3* and the triple mutant *rem1.2 rem1.3 rem1.4* (**Figure 4 – figure supplement 1**). We did not notice any obvious defects in the growth and development of seedlings and adult plants for the single, double and triple mutants, when grown under our conditions (**Figure 4 – figure supplement 2**). No difference in PLAMV-GFP propagation could be observed in the single mutants, compared to Col-0 (**Figure 4A**). However, the double mutant *rem1.2 rem1.3* showed a significant increase of infection foci area compared to Col-0, which was further enhanced in *rem1.2 rem1.3 rem1.4* triple KO mutant. Such additive effect of multiple mutations shows that REM1.2, REM1.3 and REM1.4 are functionally redundant regarding PLAMV cell-to-cell propagation. Finally, PLAMV-GFP systemic propagation was followed in whole plants every 3-4 days from 10 to 17 dpi and *rem1.2 rem1.3 rem1.4* displayed an increased infection surface of systemic leaves compared to Col-0 (**Figure 4B** and **C**), suggesting that group 1 REMs are involved in both local and systemic propagation of PLAMV-GFP.

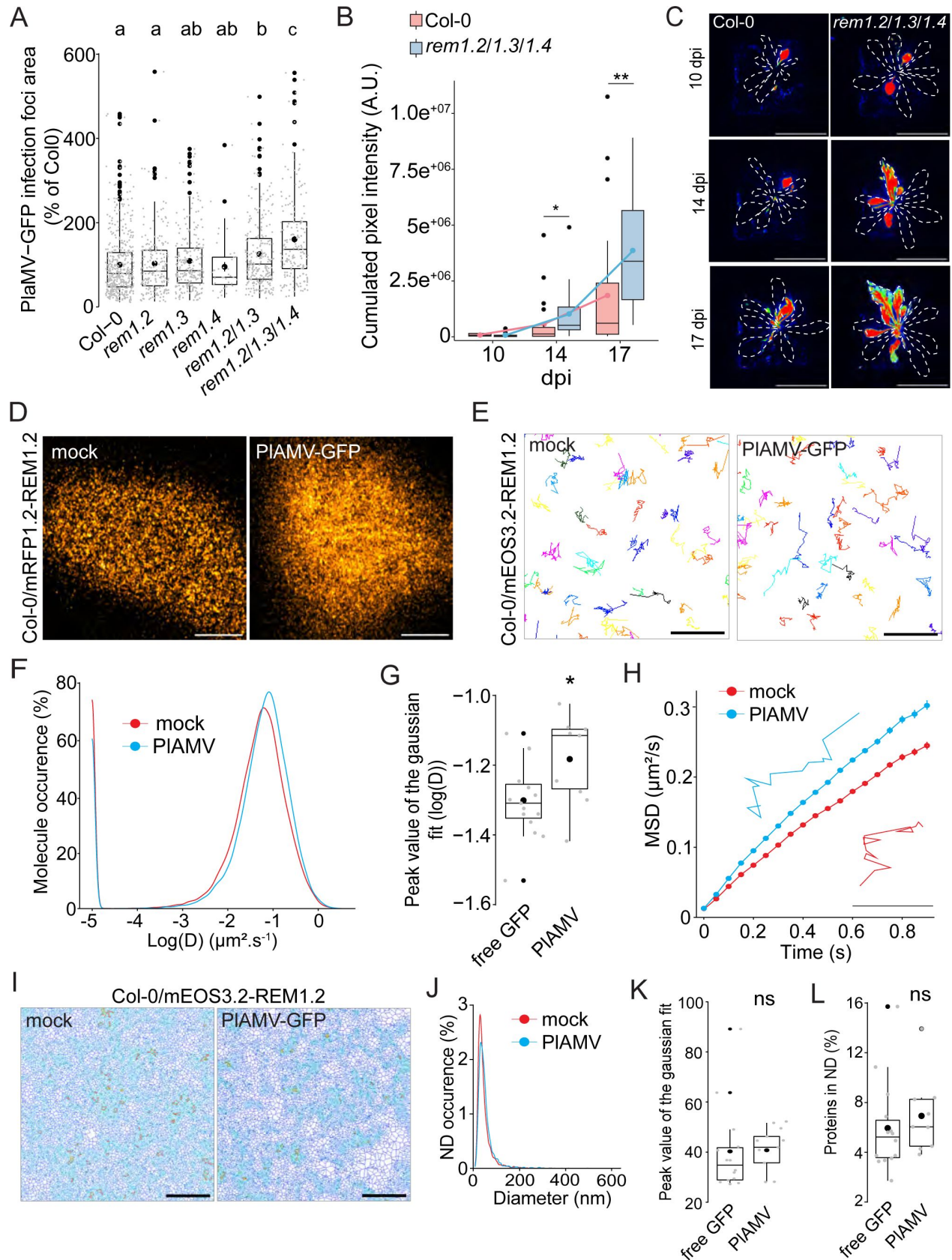


Figure 4.

Group 1 REM hampers PIAMV-GFP cell-to-cell propagation and REM1.2 diffusion increases upon infection

A. Box plots of the mean area of PIAMV-GFP infection foci in *rem1.2*, *rem1.3*, *rem1.4* single mutants along with *rem1.2 rem1.3* double mutant and *rem1.2 rem1.3 rem1.4* triple mutant. Three independent biological repeats were performed, with at least 36 foci per experiment and per genotype. Significant differences were revealed using a One-Way ANOVA followed by a Tukey's multiple comparison test. Letters are used to discriminate between statistically different conditions ($p < 0.05$).

B. Box plots of the mean cumulated intensity measured in infected leaves in Col-0 and *rem1.2 rem1.3 rem1.4* during systemic viral propagation. Two independent experiments were conducted. Statistical significance of the difference between Col-0 and *rem1.2 rem1.3 rem1.4* at each time point was assessed using a Mann-Whitney test. *: $p < 0.05$, **: $p < 0.01$

C. Representative images of *A. thaliana* plants infected with PIAMV-GFP and imaged with a CCD Camera from 10 to 17 dpi. Systemic leaves are circled with a white dotted line. Multicolored scale is used to enhance contrast and ranges from blue (low intensity) to red (high intensity). Scale bar = 4 cm.

D. Confocal images of the surface view of *A. thaliana* epidermal cells of the Col-0/ProUbi10:mRFP1.2-REM1.2, infiltrated either with free GFP ("mock") or PIAMV-GFP. Scale bar = 5 μm

E. Representative trajectories of Col-0/ProUbi10:mEOS3.2-REM1.2 five days after infiltration with free GFP ("mock") or PIAMV-GFP. Scale bar = 2 μm

F. Distribution of the diffusion coefficient (D), represented as $\log(D)$ for Col-0/ProUbi10:mEOS3.2-REM1.2 five days after infiltration with free GFP ("mock") or PIAMV-GFP. Data were acquired from at least 28638 trajectories obtained from at least 16 cells over the course of three independent experiments.

G. Box plot of the mean peak value extracted from the Gaussian fit of $\log(D)$ distribution. Significant difference was revealed using a Mann-Whitney test. *: $p < 0.05$.

H. Mean square displacement (MSD) over time of Col-0/ProUbi10:mEOS3.2-REM1.2 infiltrated either with free GFP ("mock") or PIAMV-GFP. Representative trajectories extracted from [Figure 4E](#) illustrate each curve. Scale bar = 1 μm .

I. Voronoi tessellation illustration of Col-0/ProUbi10:mEOS3.2-REM1.2 five days after infiltration with free GFP ("mock") or PIAMV-GFP. ND are circled in red. Scale bar = 2 μm

J. Distribution of the ND diameter of Col-0/ProUbi10:mEOS3.2-REM1.2 five days after infiltration with free GFP ("mock") or PIAMV-GFP.

K. Box plot representing the mean peak value of ND diameter extracted from the Gaussian fit of [Figure 4J](#). No significant difference was revealed using a Mann-Whitney test.

L. Boxplot of the proportion of Col-0/ProUbi10:mEOS3.2-REM1.2 detections found in ND five days after infiltration with free GFP ("mock") or PIAMV-GFP. No significant difference was revealed using a Mann-Whitney test.

Given their role in cell-to-cell viral movement, we checked whether group 1 REM expression was modified upon infection. RT-qPCR and western blots showed that neither transcripts nor protein levels were modified upon PIAMV infection (Figure 4 – figure supplement 3). Since REM1.2 and REM1.3 share a large part of their interactome and show functional redundancy regarding PIAMV

infection, we decided to focus on REM1.2 for further investigations. Confocal imaging of the surface of epidermal cells of Col-0/ProUbi10:mRFP1.2-REM1.2 showed a rather heterogeneous distribution at the PM, although less striking than previously described when observed in root³¹ (Figure 4D). REM1.2 was next fused to mEOS3.2 and stably expressed in Col-0 to conduct spt-PALM (Figure 4E). The diffusion coefficient of ProUbi10:mEOS3.2-REM1.2 was significantly increased upon PLAMV infection (Figure 4F and G). Moreover, its MSD was increased to a similar extent as what was previously observed with StREM1.3 during a PVX infection¹⁵ (Figure 4H), although REM1.2 is overall more mobile than StREM1.3. Tessellation analysis of protein localization did not show any difference in ND organization, whether in size or regarding the enrichment of proteins in ND (Figure 4I-L).

Taken together, these results show that group 1 REMs are functionally redundant regarding their ability to hamper PLAMV propagation. PLAMV infection promoted an increased diffusion of REM1.2, in the same way as PVX did with StREM1.3. The conservation of such mechanism between plants of different families is indicative of its physiological importance.

PLAMV-induced changes in REM1.2 and CPK3 plasma membrane dynamics are interdependent

Group 1 REMs from *A. thaliana* were previously identified as *in vitro* substrates of CPK3¹⁹. Moreover, untargeted immunoprecipitation experiments coupled to mass spectrometry identified CPK3 as an interactor of REM1.2 in *A. thaliana*⁴⁵. We wanted to assess the functional link between CPK3 and group 1 REM in potexvirus propagation by knocking out CPK3 into the *rem1.2 rem1.3 rem1.4* mutant background. We isolated two independent CRISPR-generated *rem1.2 rem1.3 rem1.4 cpk3* #1 and *rem1.2 rem1.3 rem1.4 cpk3* #2 quadruple mutants (Figure 5 – figure supplement 1). We did not observe any developmental defect in these lines when grown under controlled conditions (Figure 5 – figure supplement 2). The analysis of PLAMV-GFP propagation showed that no significant additive effect could be observed between the quadruple mutant lines, *cpk3-2* and *rem1.2 rem1.3 rem1.4* (Figure 5A and 5B). This indicates that group 1 REMs and CPK3 function in the same signaling pathway to inhibit PLAMV propagation.

We wanted to know whether the increased diffusion of REM1.2 observed on PLAMV infection was dependent on CPK3. Using spt-PALM, we obtained the diffusion parameters of ProUbi10:REM1.2-mEOS3.2 expressed in the *cpk3-2* mutant background. Strikingly, we observed that both the diffusion coefficient and MSD of REM1.2 were not anymore affected during a viral infection (Figure 5C-F), showing that REM1.2 PM lateral diffusion upon PLAMV infection depends on CPK3. In a similar manner as in Col-0, REM1.2 clustering upon PLAMV infection in *cpk3-2* background did not display any difference to the mock-infected plants (Figure 5 – figure supplement 3).

Moreover, we wondered whether the reciprocal effect was true for the diffusion of CPK3 in the absence of group 1 REMs. Similarly, the diffusion coefficient and the MSD of mEOS3.2-CPK3 in *rem1.2 rem1.3 rem1.4* triple KO background remained the same during an infection compared to control condition (Figure 5G-J), unlike what was observed in a Col-0 background (Figure 2D-G). This result indicated that the confinement of CPK3 proteins upon viral infection depended on the presence of group 1 REMs. Moreover, contrarily to the Col-0 background, the *rem1.2 rem1.3 rem1.4* displayed reduced protein concentration upon PLAMV infection (Figure 5 – figure supplement 3). This showed that group 1 REMs might play a role in CPK3 domain regulation upon viral infection.

As CPK3^{CA} was shown to inhibit potexvirus propagation more efficiently than the full-length protein¹⁵, we tested CPK3^{CA} ability to alter REM diffusion (Figure 5 – figure supplement 4). Upon transient co-expression with CPK3^{CA}, REM diffusion was significantly increased. As shown in

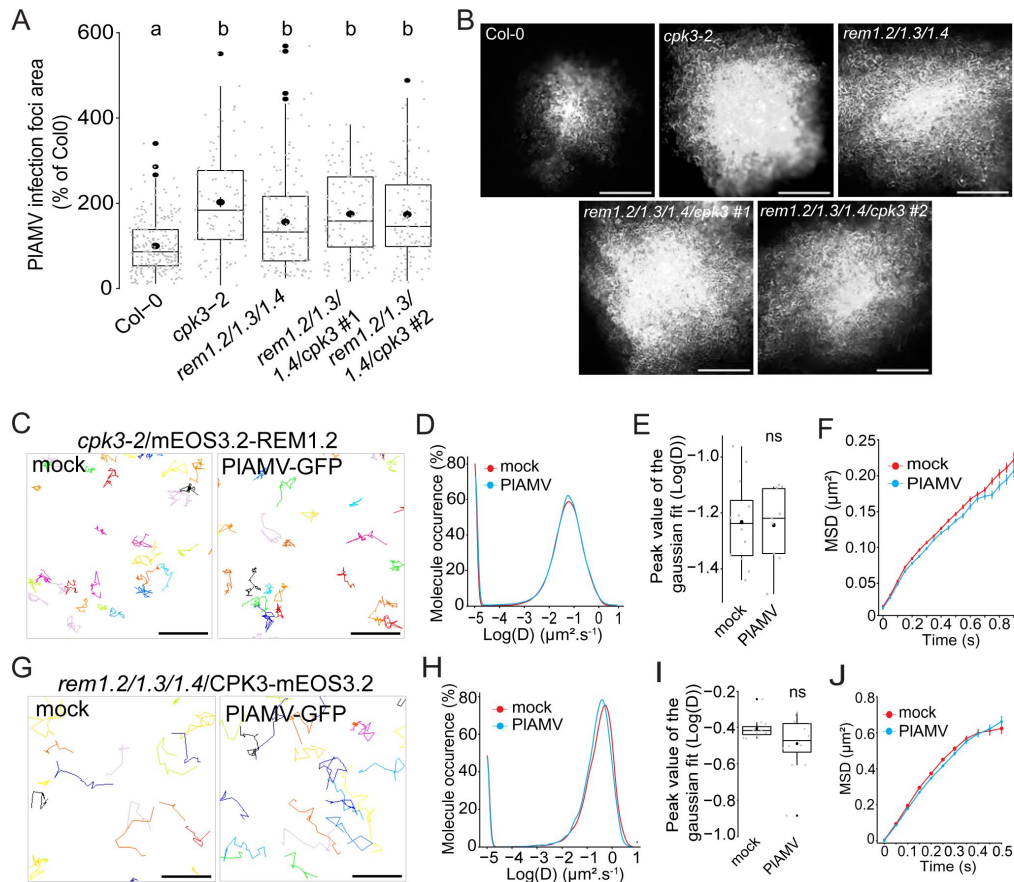


Figure 5.

Group 1 REMs and CPK3 are in the same functional pathway and regulate each other PM diffusion upon PIAMV infection

A. Box plots of the mean area of PIAMV-GFP infection foci in *cpk3-2*, *rem1.2 rem1.3 rem1.4* triple mutant and *rem1.2 rem1.3 rem1.4/cpk3 #1* and *#2* quadruple mutants. Three independent biological repeats were performed, with at least 23 foci per experiment and per genotype. Significant differences were revealed using a One-Way ANOVA followed by a Tukey's multiple comparison test. Letters are used to discriminate between statistically different conditions ($p < 0.0001$).

B. Representative images of PIAMV-GFP infection foci at 5 dpi in the different mutant backgrounds. Scale bar = 500 μ m.

C. Representative trajectories of *cpk3-2/ProUbi10:mEOS3.2-REM1.2* five days after infiltration with either free GFP ("mock") or PIAMV-GFP. Scale bar = 2 μ m.

D. Distribution of the diffusion coefficient (D), represented as $\log(D)$ for *cpk3-2/ProUbi10:mEOS3.2-REM1.2* five days after infiltration with either free GFP ("mock") or PIAMV-GFP. Data were acquired from at least 20462 trajectories obtained from at least 11 cells over the course of three independent experiments.

E. Box plot representing the mean peak value extracted from the Gaussian fit of the distribution of the diffusion coefficient (D) represented in **Figure 5D**. No significant difference was revealed using a Mann-Whitney test.

F. Mean square displacement (MSD) over time of *cpk3-2/ProUbi10:mEOS3.2-REM1.2* five days after infiltration with free GFP ("mock") or PIAMV-GFP.

G. Representative trajectories of *rem1.2 rem1.3 rem1.4/ProUbi10:CPK3-mEOS3.2* five days after infiltration with free GFP ("mock") or PIAMV-GFP. Scale bar = 2 μ m.

H. Distribution of the diffusion coefficient (D), represented as $\log(D)$ for *rem1.2 rem1.3 rem1.4/ProUbi10:CPK3-mEOS3.2* five days after infiltration with free GFP ("mock") or PIAMV-GFP. Data were acquired from at least 11724 trajectories obtained from at least 10 cells over the course of three independent experiments.

I. Box plot representing the mean peak value extracted from the Gaussian fit of the distribution of the diffusion coefficient (D) represented in **Figure 5H**. No significant difference was revealed using a Mann-Whitney test.

J. Mean square displacement (MSD) over time of *rem1.2 rem1.3 rem1.4/ProUbi10:CPK3-mEOS3.2* five days after infiltration with free GFP ("mock") or PIAMV-GFP.

Figure 2B, CPK membrane anchor is crucial for its role in viral propagation. We tested if CPK3^{CA-G2A} was still able to hinder REM diffusion, which was not the case. All these data support a specific role of PM-bound CPK3 in REM increased diffusion upon viral infection.

We then investigated whether CPK3 and REM would colocalize in absence or presence of the virus. Using confocal microscopy, we showed that they randomly colocalized in both situations (Figure 5 – figure supplement 5), the interaction between the kinase and its substrate probably occurring in a narrow spatiotemporal window.

Taken all together, those results show a strong inter-dependence of group 1 REMs and CPK3 both in their physiological function and in their PM lateral diffusion upon PIAMV infection.

Discussion

CPK3 specific role in viral immunity is supported by its PM organization

Although calcium-mediated signaling is suspected to be involved in viral immunity, only few calcium-modulated proteins are described as playing a role in viral propagation^{15,46}. We showed here the crucial role of CPK3 over other immunity-related CPK isoforms^{24,25} by a reverse genetic approach in *Arabidopsis*. The precise role of CPK3 in viral immunity remains to be determined. CPK3 phosphorylates actin depolymerization factors to modulate the actin cytoskeleton^{21,47}, a key player in host-pathogen interaction⁴⁸. In particular, potexviruses induce the remodeling of the actin cytoskeleton to organize the key steps of their cycle, whether it is replication, intra-cellular movement or cell-to-cell propagation^{49,50}. PIAMV replication and/or movement could be affected by CPK3-mediated alteration of the cytoskeleton mesh.

The specificity of a calcium-dependent kinase in a given biological process is determined by its expression pattern, subcellular localization and substrate specificity²⁷. Controlled subcellular localization ensures proximity with either stimulus or substrate and here we showed that, similarly to *Arabidopsis* CPK6⁵² and *Solanum tuberosum* CPK5⁵³, the disruption of CPK3 membrane anchor led to a loss-of-function phenotype (**Figure 2B**). Interestingly, we observed a reduction in CPK3 PM diffusion upon PIAMV infection, suggesting that not only membrane localization but also protein organization at the PM is important during viral immunity. Moreover, PIAMV-induced CPK3 PM confinement was reminiscent of the diffusion parameters displayed by CPK3^{CA}, hinting that viral infection, kinase activation and lateral diffusion are linked. However, it is necessary to remain careful as a truncated protein deprived of its auto-inhibitory domain does not reflect the controlled and context-dependent activation of CPK3. Indeed, stable expression of CPK3^{CA} was previously shown to be lethal³⁷. CPK3^{CA} ever-activated state might lead to stable or unspecific interaction with protein partners along with erratic phosphorylation of substrates, which could explain the PM domains formed by CPK3^{CA} at the PM.

CPK3 nanoscale dynamics upon viral infection might offer another layer of specificity to convey the appropriate response to a given stimulus by ensuring proximity with specific regulators or substrates. It would be interesting to explore whether the reduction of CPK3 diffusion observed upon PIAMV infection is specific to this virus or if it can be extended to other viral species, genera and even pathogens. Indeed, it was recently shown that CPK3 transcription was enhanced upon infection by viruses from different genera⁵⁴. Moreover, CPK3 regulates herbivore responses by phosphorylating transcription factors²⁰, is activated by flg22 in protoplasts¹⁹ and is proposed to be the target of a bacterial effector to disrupt immune response²¹. Finally, the diffusion and clustering of other PM-localized CPKs could be investigated as no experimental data exist yet regarding their PM nano-organization. It would be especially relevant to describe these parameters for the CPK isoforms phosphorylating ND-organized NADPH oxidases^{14,25,28}.

Potential functions for REM1.2 increased diffusion upon PIAMV

REM proteins display a wide range of physiological functions and are proposed to function as scaffold proteins^{43,44,55}. Group 1 REMs have been shown to be involved in viral immunity, playing apparent contradictory roles depending on the virus genera^{8,44,56}. Herein, we show through a combination of genetic and biochemical analysis that the three most expressed isoforms of group 1 *Arabidopsis* REMs were functionally redundant in inhibiting PIAMV propagation (Figure 4A). REMs are anchored at the PM through their C-terminal sequence^{44,56,58} but despite displaying a similar PM attachment, potato StREM1.3 is static and forms well defined membrane compartments⁵⁷ while *Arabidopsis* REM1.2 appeared mobile in leaves, with small and potentially short-lived membrane domains of around 70nm (Figure 4F-J). Beyond clear organizational differences, both REM1.2 and StREM1.3 showed an increased mobility upon viral infection in *N. benthamiana* and *Arabidopsis*¹⁵ (Figure 4E-H), which is at contrast with the canonical model linking protein activation with its stabilization into ND^{11,59}. Particularly, REM1.2 was recently shown to form ND upon elicitation by a bacterial effector¹³ or upon exposition to bacterial membrane structures⁶⁰. Conservation across plant and virus species of such increased PM diffusion of group 1 REMs indicates that this specific mechanism is crucial for plant response to potexviruses, although its role remains to be deciphered. It was suggested, in the context of tobacco rattle virus infection, that REM1.2 clusters led to an increased lipid order of the PM and a morphological modification of plasmodesmata (PD), inducing a decrease of PD permeability³¹. As REM1.2 does not accumulate at PD upon PIAMV infection (Figure 4 – figure supplement 4), it might indirectly influence PD permeability through mechanisms yet to be discovered. We previously showed that StREM1.3 modulated the formation of lipid phases *in vitro*⁶¹ while *Medicago truncatula* SYMREM1 was recently shown to stabilize membrane topology changes in protoplasts⁶¹. Therefore, REM1.2 increased diffusion upon viral infection might alter lipid organization, with consequences on PM and PD-localized proteins⁶². Based on REM's putative scaffolding role^{43,63}, its increased PM diffusion might modify the stability of REM-supported complexes and induce subsequent signaling, similarly to the way *Oryza sativa* REM4.1 orchestrates the balance between abscisic acid and brassinosteroid pathways by interacting with different protein kinases⁶⁴.

A PM-localized mechanism involved in hampering viral propagation

Increasing evidence supports the role of PM proteins in plant antiviral mechanism⁶⁵. However, while the nano-organization of PM proteins involved in bacterial or fungal immunity begins to be addressed^{13,60,66,67}, there is still only scarce information in a viral infection context. Our observations pointed towards an interdependence of REM and CPK3 in their PM diffusion upon PIAMV infection. In particular, CPK3-dependent REM increased diffusion in a potexvirus infection is consistent with our previously reported PM diffusion increase of StREM1.3 phosphomimetic mutant, reminiscent of StREM1.3 behavior upon viral infection¹⁵. Moreover, we recently published that *in vitro* CPK3-phosphorylated StREM1.3 presented disrupted domains on model membranes compared to the non-phosphorylated protein¹⁶. The data presented in this paper further support the predominant role of CPK3 in viral-induced REM1.2 diffusion (Figure 5C-F). Since the actin cytoskeleton was shown to favor nanometric scale ND including those of group 1 REM⁶⁸, CPK3 mediated regulation of the actin cytoskeleton could regulate REM1.2 PM nanoscale organization. We also discovered the essential role of group 1 REMs in the lateral organization of CPK3 upon viral infection (Figure 5G-J), which is further supported by the difference between CPK3 clustering parameters when expressed in *N. benthamiana* or in *Arabidopsis*: CPK3 was enriched in ND upon PIAMV infection when transiently expressed in *N. benthamiana* but not in *Arabidopsis* (Figure 2H, 2K, 3F and 3I). The discrepancy between both species could be linked to *N. benthamiana* REM1 ability to form stable ND, discernable by confocal microscopy⁵ while we observed small and unstable domains of REM1.2 in *Arabidopsis* leaves (Figure 4I-K). Moreover, CPK3 ND organization was disrupted in *rem1.2 rem1.3 rem1.4* triple KO background

upon PLAMV infection (Figure 5 – figure supplement 3H), indicating that group1 REMs are crucial for the spatial organization of CPK3 during a viral infection. Furthermore, the sensitivity of CPK3^{CA} domains to the same lipid inhibitors as StREM1.3⁵⁷ (Figure 3J,K) hints that REM1.2 lipid environment might be required for CPK3 nanoscale organization.

Although the data obtained here do not allow us to determine the sequence of events orchestrating REM1.2 and CPK3 dynamic interaction, hypotheses can be formulated (Figure 6). REM and CPK3 interact in the absence of any stimulus^{15,45} but as they display drastically different diffusion parameters (Figure 2E, Figure 4F), likely only a small part of proteins interact at basal state. PLAMV infection induces a REM-dependent confinement of CPK3 (Figure 2 and Figure 5). Whether CPK3 confinement is concomitant to its activation remains to be confirmed. Such modification of CPK3 mobility might result in an increase probability of interaction with REM1.2, which might lead to increased phosphorylation events and a subsequent increase in mobility of REM1.2. In addition to the above-mentioned putative roles of REM's increased diffusion, such “kiss-and-go” mechanism between a kinase and its substrate might also be considered as a negative feedback loop to hamper constitutive activation of the system. It was recently shown that the PM organization of a receptor-like kinase and its co-receptor relied on the expression of a scaffold protein^{67,69}, REM might go beyond the role of substrate and be essential to maintain the required PM environment of its cognate kinase to ensure proper signal transduction. Although the complexity of potexvirus' lifecycle as well as technical limitations impair a thorough challenge of this hypothesis, our data support the significance of fine PM compartmentalization and spatio-temporal dynamics in signal transduction upon viral infection in plants while it explores new concepts underlying plant kinases PM organization.

Acknowledgements

We thank Thierry Mauduit and Christophe Higelin (HPE Greenhouse, INRAe) for plant culture. We thank the Bordeaux Imaging Center, part of the National Infrastructure France-BioImaging supported by the French National Research Agency (ANR-10-INBS-04). This work was supported by the French National Research Agency (grant no. ANR-19-CE13-0021 to SGR, SM, VG, MB) and the German Research Foundation (DFG) grant CRC1101-A09 to JG, the IPS2 benefits from the support of the LabEx Saclay Plant Sciences-SPS (ANR-10-LABX-0040-SPS). This study received financial support from the French government in the framework of the IdEX Bordeaux University “Investments for the Future” program / GPR “Bordeaux Plant Sciences”.

Additional information

Authors contribution

Conceptualization: M.-D.J., S.M, V.G.

Investigation: M-D. J, A.-F. D., M.B., N.B.A., M.R., T.R., V. W.-B., J.H., D.L., G.S., J.A

Resources: M.-D.J., M.B., V.W.-B., J.H., D.L., N.B.A., Y.-J.L., B.D., V.C., N.G., J.-L.G., Y.Y. T.O.

Writing (Original Draft): M.-D.J., S.M.

Writing (Review and Editing): M.-D.J., M.B., N.A., V.W.-B., J.A., V.C., J.-L.G., S.G.-R., J.G., S.M, V.G.

Visualization: M.D.J, A-F.D.

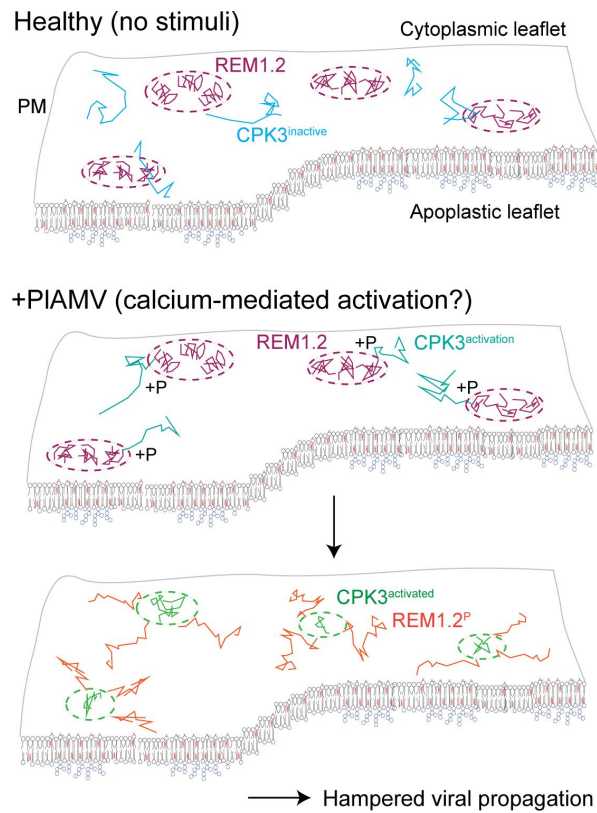


Figure 6.

Proposed “kiss-and-run” model describing REM1.2 and CPK3 interdependence

In healthy conditions, REM1.2 displays a smaller mobility at the PM than CPK3. Random interactions between the two proteins can occur.

Upon PIAMV infection, CPK3 shows a REM-dependent confined behavior which might be concomitant to its activation. Simultaneously, a PIAMV infection leads to a CPK3-dependent increased diffusion of REM1.2, which might be a consequence of its phosphorylation by CPK3.

Funding acquisition: S.M., V.G., S.G.-R., T.O.

Declaration of interests

The authors declare no competing interests

Material and methods

Plant culture

Nicotiana benthamiana plants were cultivated in controlled conditions (16 h photoperiod, 25 °C). Proteins were transiently expressed via *Agrobacterium tumefaciens* as previously described⁵⁷. The agrobacteria GV3101 strain was cultured at 28°C on appropriate selective medium depending on constructs carried. Plants were observed between 2 and 5 days after infiltration depending on experiments.

Sterilized *Arabidopsis thaliana* seeds were germinated on ½ MS plates supplemented with 1% sucrose. 10-day-old seedlings were transferred to soil and grown under short day conditions (8 h light/ 16 h dark).

Cloning

REM1.2, CPK3 and CPK3^{CA} sequences were previously published¹⁵. CPK3^{K107M} was generated by site-directed mutagenesis using CPK3 as a template and primers specified in the Supplemental Table 1.

All vectors built for this project, except for CRISPR and some protein production, were generated using multisite Gateway cloning strategies (www.lifetechnologies.com) with pDONR P4-P1r, pDONR P2R-P3, pDONR221 as entry vectors. pLOK180_pR7m34g⁷¹ was used as a destination vector for plant expression. pGEX-2T (GE Healthcare, N-terminal fusion with GST) was used for CPK protein production in bacteria for previously reported constructs⁷² (CPK2/3/5/11). CPK1, CPK3^{K107M} and CPK6 were cloned into pGEX-3X-GW using the gateway cloning system and pDONR207 as entry vector. The N-terminal 118 amino acids of REM1.2 (REM1.2¹⁻¹¹⁸) was synthesized with optimized codons for bacterial expression by GenScript (gencript.com) and cloned into pET24a (C-terminal fusion with a 6-histidine tag) between Nde1 and XhoI.

To generate CRISPR lines, sgRNAs targeting the N-terminus of *CPK3* gene were selected using CRISPR-P 2.0 website⁷³ (<http://crispr.hzau.edu.cn/CRISPR2>) and cloned into pHEE401 backbone⁷⁴ carrying the gene coding for the zCas9 enzyme under the control of Egg cell promoter using the Golden Gate cloning method.

All constructs were propagated using the NEB10 *E. coli* strain (New England Biolabs). Primers used for cloning are detailed in Supplemental Table 1.

Plant lines generation

T-DNA insertion mutants *rem1.2* (salk_117637.50.50.x), *rem1.3* (salk_117448.53.95.x) and *rem1.4* (SALK_073841.47.35) were provided by the ABRC. *rem1.2 rem1.3* double mutant was generated by crossing the respective T-DNA inserted parental plants, *rem2/rem1.3/rem1.4* was created by crossing *rem1.2 rem1.3* with *rem1.4*. The *cpk5 cpk6* (sail_657_C06, salk_025460) and *cpk5 cpk6 cpk11* (sail_657_C06, salk_025460, salk_054495) were described previously²⁴. The quadruple mutant *cpk3 cpk5 cpk6 cpk11* was described previously²⁶. *cpk1 cpk2* (salk_096452, salk_059237) and *cpk1 cpk2 cpk5 cpk6* (salk_096452, salk_059237, sail_657_C06, salk_025460) were described previously²⁵. CPK3 T-DNA insertion lines *cpk3-1* (salk_107620) and *cpk3-2* (salk_022862) were

obtained from Julian Schroeder³² and Bernhard Wurzing¹⁹, respectively. All mutants are in the same genetic ecotype Columbia Col-0. All plants were genotyped using primers indicated in the Supplemental Table 1.

Pro35S:CPK3-HA #16.2, *cpk3-2*/Pro35S:CPK3-myc and *cpk3-2*/Pro35S:CPK3^{K107M}-myc used for viral propagation were previously published^{21,72}. Pro35S:CPK3-HA #8.2 was generated at the same time as Pro35S:CPK3-HA #16.2, and protein expression was confirmed (Figure 1 – figure supplement 3).

Col-0 plants were floral dipped with either ProUbi10:CPK3-mRFP1.2, ProUbi10:CPK3-mEOS3.2 or ProUbi10:mEOS3.2-REM1.2. *cpk3-2* plants were floral dipped with either ProUbi10:CPK3-mRFP1.2, ProUbi10:CPK3^{G2A}-mRFP1.2 or ProUbi10:mEOS3.2-REM1.2. *rem1.2 rem1.3 rem1.4* plants were floral dipped with ProUbi10:CPK3-mEOS3.2. Col-0/ProREM1.2:YFP-REM1.2⁷⁵ was transformed with ProUbi10:CPK3-mTagBFP2. Transformed seeds were selected based on the seedcoat RFP fluorescence.

For CRISPR-mediated site mutagenesis of CPK3, *rem1.2 rem1.3 rem1.4* was transformed by floral dip with the plasmid carrying *zCas9* encoding gene and the sgRNA. Transformed candidates were selected on hygromycin and grown for seed collection. Harvested seeds were grown and a leaf sample was harvested for genomic DNA extraction. PCR were performed to amplify the targeted region, and CRISPR-induced mutations were screened using capillary electrophoresis. Mutated candidates were sent to sequencing to obtain homozygous lines for the mutation and then backcrossed with *rem1.2 rem1.3 rem1.4* to remove the Cas9. Primers used for CRISPR screening are listed in Supplemental Table 1.

Local viral propagation assay

Viral propagation assays were performed using PIAMV-GFP, an agroinfiltrable GFP-tagged infectious clone of PIAMV²². *Agrobacterium tumefaciens* strain GV3101 carrying PIAMV-GFP was infiltrated on 3-week-old *A. thaliana* plants at $OD_{600nm} = 0.2$. Viral spreading was tracked using Axiozoom V16 microscope system 5 days after infection. Infection foci were automatically analyzed using the Fiji software (<http://www.fiji.sc/>) via a homemade macro. The statistical significance was assessed using a two-way ANOVA, followed by a Tukey's multiple comparison test.

Systemic viral propagation assay

At 3-week-old, leaves were infiltrated with *Agrobacterium tumefaciens* GV3101 strain carrying PIAMV-GFP vector. Infection was followed every three-four days from the 10th day of infection to the 17th using a closed GFP-CAM FX 800-0/1010 GFP camera and the Fluorcam7 software (Photon System Instruments, Czech Republic; <https://fluorcams.psi.cz/>). Image analysis was performed using Fiji software (<https://fiji.sc/>). Integrated density of the fluorescence of systemic leaves was measured. Two independent experiments with at least 30 plants per genotype were performed. Statistical significance was determined with a Mann-Whitney test or a Kruskal-Wallis followed by a Dunn's multiple comparison test, depending on the number of conditions.

Confocal microscopy

Live imaging was performed using a Zeiss LSM 880 confocal laser scanning microscopy system using either an oil-immersion PL-APO 40x or 68x (NA = 1.4) objective coupled with an AiryScan detector for the latter. mRFP1.2 fluorescence was observed using an excitation wavelength of 561 nm and an emission wavelength of 579 nm. Acquisition parameters remained the same across experiments for SCI quantification. The SCI was calculated as previously described⁵⁷. Briefly, 10 μ m lines were plotted across the samples and the SCI was calculated by dividing the mean of the

5% highest values by the mean of 5% lowest values. Three lines were randomly plotted per cell. Three independent experiments were done, on at least 10 cells each time. Fenpropimorph (10 μ g/mL) or DMSO was infiltrated 24 hours before observation.

spt-PALM microscopy

N. benthamiana and *A. thaliana* epidermal cells were imaged at RT. Samples of leaves of 3-week-old plants stably or transiently expressing mEOS3.2-tagged constructs were mounted between a glass slide and a cover slip in a drop of water to avoid dehydration. With the exception of ProUbi10:mEOS3.2-REM1.2 transiently expressed in *N. benthamiana*, image acquisitions were done on an inverted motorized microscope Nikon Ti Eclipse equipped with a 100 \AA ~ oil-immersion PL-APO objective (NA = 1.49), a TIRF arm and a sCMOS Camera FUSION BT (Hamamatsu). Laser angle was adjusted to obtain the highest signal-to-noise ratio while laser power of a 405nm and 561nm laser, respectively to activate and image mEOS3.2, was adjusted to obtain a sufficient concentration of individual particles. Particle localization, tracks reconstructions, diffusion coefficient and MSD parameters were obtained using PALMtracer, as previously described⁵⁷. The diffusion coefficient was calculated from the four first points of the MSD. Three independent experiments were conducted for each tested condition. Tessellation analysis was conducted using SR-Tesseler as previously described^{34,57}. ND were considered to be at least 32 nm², to contain at least 5 particles and to have a particle density twice the average particle density within the sample.

For ProUbi10:mEOS3.2-REM1.2 transiently expressed in *N. benthamiana* in the presence or absence of ProUbi10:CPK3^{CA}-mVenus or ProUbi10:CPK3^{CAG2A}-mVenus, images were acquired on a custom-built platform, as described previously⁷⁶. Particle localization, tracks reconstructions, diffusion coefficient and MSD parameters were obtained using OneFlowTraX⁷⁶. Particle localization was done using the following parameters: photon/ADU conversion of 0.48, an offset of 100, a pixel size of 100 nm, a filter size of 1.2, a cut-off of 3 and a PSF of 7. Track reconstruction was done with a maximum linking distance of 200 nm, a maximum gap frame of 4. Tracks smaller than 8 localizations were filtered out and the diffusion coefficient was calculated from the 2nd to 5th data points.

RT-qPCR

3-week-old *A. thaliana* leaves were infiltrated with PIAMV-GFP at final OD_{600nm} = 0.2. Leaf samples were harvested 7 days after infiltration and immediately frozen. RNA extraction was done using Qiagen Plant Mini Kit and was followed by a DNase treatment. cDNA was produced from the extracted RNA using Superscript II enzyme from Invitrogen. RT-qPCR was performed on obtained cDNA using the iQTM SYBR[®] Green supermix (BioRad) on the iQ iCycler thermocycler (BioRad). The transcript abundance in samples was determined using a comparative threshold cycle method and was normalized to actin expression. Statistical differences were determined using a Mann-Whitney test. Primers used for RT-qPCR are listed in Supplemental Table 1.

Production of recombinant proteins and *in vitro* kinase assay

GST-CPK proteins were produced in BL21(DE3)pLys and purified as previously reported⁷². 6His-AtREM1.2¹⁻¹¹⁸ was produced like GST-CPK and purified on Protino[®] Ni-TED column following manufacturer's instructions (Macherey-Nagel). After elution with 40-250 mM imidazole, proteins were dialyzed overnight in 30 mM Tris HCl pH 7.5, 10% glycerol. Kinase assay was performed as previously described¹⁵ using 400 ng recombinant GST-CPK and 1-2 μ g substrate (6His-AtREM1.2¹⁻¹¹⁸ or histone).

Production of CPK3 antibodies

Polyclonal antibodies against *Arabidopsis* CPK3 were raised in rabbit by Covalab (France) using purified recombinant GST-CPK3. The antibodies were purified from rabbit serum by affinity chromatography on CH-Sepharose 4B (GE Healthcare) coupled to 6His-CPK3. To produce the recombinant 6His-CPK3 and GST-CPK3 proteins, the *Arabidopsis* CPK3 cDNA was cloned into the expression vectors pDEST17 and pDEST15 (Invitrogen), respectively. Expression of 6His-CPK3 was induced in *Escherichia coli* strain BL21-AI (Invitrogen) with 0.2% (m/v) arabinose and the recombinant protein was affinity purified using Ni-NTA agarose (Qiagen). For GST-CPK3, protein expression in *E. coli* Rosetta cells (Novagen) was induced with 0.5 mM IPTG (isopropyl- β -D-thiogalactopyranoside) and recombinant GST-CPK3 was purified by Glutathione Sepharose 4 Fast Flow chromatography (GE Healthcare) as described by the manufacturer.

Western Blots

Protein samples were extracted from *A. thaliana* leaf tissue using 2X Laemmli buffer or in a buffer containing 50 mM Tris HCl pH 7.5, 5 mM EDTA, 5 mM EGTA, 1X anti-protease cocktail [Roche], 1% Triton X-100, 2 mM DTT. Proteins were transferred to PVDF and detected with polyclonal antibodies raised against CPK3 or REM1.2/REM1.3⁶², followed by incubation with secondary anti-rabbit HRP-conjugated antibodies (Sigma).

References

1. Hanssen I.M., Thomma B.P.H.J (2010) **Pepino mosaic virus: a successful pathogen that rapidly evolved from emerging to endemic in tomato crops** *Mol. Plant Pathol* **11**:179–189 <https://doi.org/10.1111/J.1364-3703.2009.00600.X>
2. Zorzatto C. *et al.* (2015) **NIK1-mediated translation suppression functions as a plant antiviral immunity mechanism** *Nature* **520** <https://doi.org/10.1038/NATURE14171>
3. Ngou B.P.M., Ding P., Jones J.D.G (2022) **Thirty years of resistance: Zig-zag through the plant immune system** *Plant Cell* **34**:1447–1478 <https://doi.org/10.1093/PLCELL/KOAC041>
4. Cheng G., Yang Z., Zhang H., Zhang J., Xu J (2020) **Remorin interacting with PCaP1 impairs Turnip mosaic virus intercellular movement but is antagonised by VPg** *New Phytol* **225**:2122–2139 <https://doi.org/10.1111/NPH.16285>
5. Fu S., Xu Y., Li C., Li Y., Wu J., Zhou X (2018) **Rice Stripe Virus Interferes with S-acylation of Remorin and Induces Its Autophagic Degradation to Facilitate Virus Infection** *Mol. Plant* **11**:269–287 <https://doi.org/10.1016/j.MOLP.2017.11.011>
6. Ma T., Fu S., Wang K., Wang Y., Wu J., Zhou X (2022) **Palmitoylation Is Indispensable for Remorin to Restrict Tobacco Mosaic Virus Cell-to-Cell Movement in Nicotiana benthamiana** *Viruses* **14** <https://doi.org/10.3390/V14061324>
7. Raffaele S. *et al.* (2009) **Remorin, a solanaceae protein resident in membrane rafts and plasmodesmata, impairs potato virus X movement** *Plant Cell* **21**:1541–1555 <https://doi.org/10.1105/tpc.108.064279>
8. Rocher M., Simon V., Jolivet M.D., Sofer L., Deroubaix A.F., Germain V., Mongrand S., German-Retana S (2022) **StREM1.3 REMORIN Protein Plays an Agonistic Role in Potyvirus Cell-to-Cell Movement in N. benthamiana** *Viruses* **14** <https://doi.org/10.3390/V14030574>
9. Son S., Oh C.J., An C.S (2014) **Arabidopsis thaliana remorins interact with SnRK1 and play a role in susceptibility to beet curly top virus and beet severe curly top virus** *Plant Pathol. J* **30**:269–278 <https://doi.org/10.5423/PPJ.OA.06.2014.0061>
10. Gronnier J., Gerbeau-Pissot P., Germain V., Mongrand S., Simon-Plas F (2018) **Divide and Rule: Plant Plasma Membrane Organization** *Trends Plant Sci* **23**:899–917 <https://doi.org/10.1016/j.tplants.2018.07.007>
11. Jaillais Y., Ott T (2020) **The nanoscale organization of the plasma membrane and its importance in signaling: A proteolipid perspective** *Plant Physiol* **182**:1682–1696 <https://doi.org/10.1104/PP.19.01349>
12. Platre M.P. *et al.* (2019) **Developmental control of plant Rho GTPase nano-organization by the lipid phosphatidylserine** *Science (80-.)* **364**:57–62 <https://doi.org/10.1126/science.aav9959>

13. Ma Z., Sun Y., Zhu X., Yang L., Chen X., Miao Y (2022) **Membrane nanodomains modulate formin condensation for actin remodeling in Arabidopsis innate immune responses** *Plant Cell* **34**:374–394 <https://doi.org/10.1093/PLCELL/KOAB261>
14. Smokvarska M. *et al.* (2020) **A Plasma Membrane Nanodomain Ensures Signal Specificity during Osmotic Signaling in Plants** *Curr. Biol* **30**:4654–4664 <https://doi.org/10.1016/j.cub.2020.09.013>
15. Perraki A. *et al.* (2018) **REM1.3's phospho-status defines its plasma membrane nanodomain organization and activity in restricting PVX cell-to-cell movement** *PLoS Pathog* **14** <https://doi.org/10.1371/journal.ppat.1007378>
16. Legrand A. *et al.* (2022) **Structural determinants of REMORIN nanodomain formation in anionic membranes** *Biophys. J* <https://doi.org/10.1016/j.bpj.2022.12.035>
17. Martinière A., Fiche J.B., Smokvarska M., Mari S., Alcon C., Dumont X., Hematy K., Jaillais Y., Nollmann M., Maurel C (2019) **Osmotic stress activates two reactive oxygen species pathways with distinct effects on protein nanodomains and diffusion** *Plant Physiol* **179**:1581–1593 <https://doi.org/10.1104/pp.18.01065>
18. Gournas C., Gkionis S., Carquin M., Twyffels L., Tyteca D., André B (2018) **Conformation-dependent partitioning of yeast nutrient transporters into starvation-protective membrane domains** *Proc. Natl. Acad. Sci. U. S. A* **115**:E3145–E3154 <https://doi.org/10.1073/PNAS.1719462115/VIDEO-7>
19. Mehler N., Wurzinger B., Stael S., Hofmann-Rodrigues D., Csaszar E., Pfister B., Bayer R., Teige M (2010) **The Ca²⁺-dependent protein kinase CPK3 is required for MAPK-independent salt-stress acclimation in Arabidopsis** *Plant J* **63**:484–498 <https://doi.org/10.1111/j.1365-313X.2010.04257.x>
20. Kanchiswamy C.N. *et al.* (2010) **Regulation of Arabidopsis defense responses against *Spodoptera littoralis* by CPK-mediated calcium signaling** *BMC Plant Biol* **10** <https://doi.org/10.1186/1471-2229-10-97>
21. Lu Y.J., Li P., Shimono M., Corrion A., Higaki T., He S.Y., Day B (2020) **Arabidopsis calcium-dependent protein kinase 3 regulates actin cytoskeleton organization and immunity** *Nat. Commun* **11** <https://doi.org/10.1038/s41467-020-20007-4>
22. Minato N., Komatsu K., Okano Y., Maejima K., Ozeki J., Senshu H., Takahashi S., Yamaji Y., Namba S (2014) **Efficient foreign gene expression in planta using a plantago asiatica mosaic virus-based vector achieved by the strong RNA-silencing suppressor activity of TGBp1** *Arch. Virol* <https://doi.org/10.1007/s00705-013-1860-y>
23. Yamaji Y. *et al.* (2012) **Lectin-mediated resistance impairs plant virus infection at the cellular level** *Plant Cell* **24**:778–793 <https://doi.org/10.1105/tpc.111.093658>
24. Boudsocq M., Willmann M.R., McCormack M., Lee H., Shan L., He P., Bush J., Cheng S.H., Sheen J (2010) **Differential innate immune signalling via Ca²⁺ sensor protein kinases** *Nature* **464**:418–422 <https://doi.org/10.1038/nature08794>
25. Gao X. *et al.* (2013) **Bifurcation of Arabidopsis NLR Immune Signaling via Ca²⁺-Dependent Protein Kinases** *PLOS Pathog* **9** <https://doi.org/10.1371/JOURNAL.PPAT.1003127>

26. Guzel Deger A., Scherzer S., Nuhkat M., Kedzierska J., Kollist H., Brosché M., Unyayar S., Boudsocq M., Hedrich R., Roelfsema M.R.G. (2015) **Guard cell SLAC1-type anion channels mediate flagellin-induced stomatal closure** *New Phytol* <https://doi.org/10.1111/nph.13435>
27. Yip Delormel T., Boudsocq M. (2019) **Properties and functions of calcium-dependent protein kinases and their relatives in Arabidopsis thaliana** *New Phytol* **224**:585–604 <https://doi.org/10.1111/nph.16088>
28. Dubiella U., Seybold H., Durian G., Komander E., Lassig R., Witte C.P., Schulze W.X., Romeis T (2013) **Calcium-dependent protein kinase/NADPH oxidase activation circuit is required for rapid defense signal propagation** *Proc. Natl. Acad. Sci. U. S. A* **110**:8744–8749 <https://doi.org/10.1073/PNAS.1221294110/-/DCSUPPLEMENTAL>
29. Dammann C., Ichida A., Hong B., Romanowsky S.M., Hrabak E.M., Harmon A.C., Pickard B.G., Harper J.F (2003) **Subcellular targeting of nine calcium-dependent protein kinase isoforms from Arabidopsis** *Plant Physiol* **132**:1840–1848 <https://doi.org/10.1104/PP.103.020008>
30. Lu S.X., Hrabak E.M (2002) **An Arabidopsis Calcium-Dependent Protein Kinase Is Associated with the Endoplasmic Reticulum** *Plant Physiol* **128** <https://doi.org/10.1104/PP.010770>
31. Huang D. *et al.* (2019) **Salicylic acid-mediated plasmodesmal closure via Remorin-dependent lipid organization** *Proc. Natl. Acad. Sci. U. S. A* **116**:21274–21284 <https://doi.org/10.1073/pnas.1911892116>
32. Mori I.C. *et al.* (2006) **CDPKs CPK6 and CPK3 function in ABA regulation of guard cell S-type anion- and Ca²⁺-permeable channels and stomatal closure** *PLoS Biol* **4**:1749–1762 <https://doi.org/10.1371/journal.pbio.0040327>
33. Zhang M. *et al.* (2012) **Rational design of true monomeric and bright photoactivatable fluorescent proteins** *Nat. Methods* **9**:727–729 <https://doi.org/10.1038/nmeth.2021>
34. Lebet F., Hosity E., Kechkar A., Butler C., Beghin A., Choquet D., Sibarita J.B (2015) **SR-Tesseler: a method to segment and quantify localization-based super-resolution microscopy data** *Nat. Methods* **12**:1065–1071 <https://doi.org/10.1038/nmeth.3579>
35. Sheen J (1996) **Ca²⁺-dependent protein kinases and stress signal transduction in plants** *Science* **274**:1900–1902 <https://doi.org/10.1126/SCIENCE.274.5294.1900>
36. Harper J.R., Breton G., Harmon A (2004) **Decoding Ca(2+) signals through plant protein kinases** *Annu. Rev. Plant Biol* **55**:263–288 <https://doi.org/10.1146/ANNUREV.ARPLANT.55.031903.141627>
37. Huimin R., Hussain J., Wenjie L., Fenyong Y., Junjun G., Youhan K., Shenkui L., Guoning Q (2021) **The expression of constitutively active CPK3 impairs potassium uptake and transport in Arabidopsis under low K + stress** *Cell Calcium* **98** <https://doi.org/10.1016/j.CECA.2021.102447>
38. Sezgin E., Levental I., Mayor S., Eggeling C (2017) **The mystery of membrane organization: composition, regulation and roles of lipid rafts** *Nat. Rev. Mol. Cell Biol* **18**:361–374 <https://doi.org/10.1038/NRM.2017.16>
39. He J.X., Fujioka S., Li T.C., Kang S.G., Seto H., Takatsuto S., Yoshida S., Jang J.C (2003) **Sterols Regulate Development and Gene Expression in Arabidopsis** *Plant Physiol* **131** <https://doi.org/10.1104/PP.014605>

40. Simon M.L.A., Platre M.P., Marquès-Bueno M.M., Armengot L., Stanislas T., Bayle V., Caillaud M.C., Jaillais Y (2016) **A PI4P-driven electrostatic field controls cell membrane identity and signaling in plants** *Nat. plants* **2** <https://doi.org/10.1038/NPLANTS.2016.89>
41. Raffaele S., Mongrand S., Gamas P., Niebel A., Ott T (2007) **Genome-wide annotation of remorins, a plant-specific protein family: Evolutionary and functional perspectives** *Plant Physiol* **145**:593–600 <https://doi.org/10.1104/pp.107.108639>
42. Mergner J. *et al.* (2020) **Mass-spectrometry-based draft of the Arabidopsis proteome** *Nature* **579**:409–414 <https://doi.org/10.1038/S41586-020-2094-2>
43. Lefebvre B. *et al.* (2010) **A remorin protein interacts with symbiotic receptors and regulates bacterial infection** *Proc. Natl. Acad. Sci. U. S. A* **107**:2343–2348 <https://doi.org/10.1073/pnas.0913320107>
44. Gouguet P. *et al.* (2021) **Connecting the dots: From nanodomains to physiological functions of REMORINS** *Plant Physiol* **185**:632–649 <https://doi.org/10.1093/PLPHYS/KIAA063>
45. Abel N.B. *et al.* (2021) **A hetero-oligomeric remorin-receptor complex regulates plant development** *bioRxiv* <https://doi.org/10.1101/2021.01.28.428596>
46. Wang Y. *et al.* (2021) **A calmodulin-binding transcription factor links calcium signaling to antiviral RNAi defense in plants** *Cell Host Microbe* **29**:1393–1406 <https://doi.org/10.1016/j.chom.2021.07.003>
47. Dong C.H., Hong Y (2013) **Arabidopsis CDPK6 phosphorylates ADF1 at N-terminal serine 6 predominantly** *Plant Cell Rep* **32**:1715–1728 <https://doi.org/10.1007/S00299-013-1482-6>
48. Wang J., Lian N., Zhang Y., Man Y., Chen L., Yang H., Lin J., Jing Y (2022) **The Cytoskeleton in Plant Immunity: Dynamics, Regulation, and Function** *Int. J. Mol. Sci* **23** <https://doi.org/10.3390/IJMS232415553>
49. Harries P.A., Park J.-W., Sasaki N., Ballard K.D., Maule A.J., Nelson R.S. (2009) **Differing requirements for actin and myosin by plant viruses for sustained intercellular movement** *PNAS* **106**:17594–17599
50. Tilsner J., Linnik O., Wright K.M., Bell K., Roberts A.G., Lacomme C., Cruz S.S., Oparka K.J (2012) **The TGB1 movement protein of potato virus X reorganizes actin and endomembranes into the X-body, a viral replication factory** *Plant Physiol* **158**:1359–1370 <https://doi.org/10.1104/pp.111.189605>
51. Köster P., DeFalco T.A., Zipfel C (2022) **Ca²⁺ signals in plant immunity** *EMBO J* **41** <https://doi.org/10.15252/EMBJ.2022110741>
52. Saito S. *et al.* (2018) **N-myristoylation and S-acylation are common modifications of Ca²⁺-regulated Arabidopsis kinases and are required for activation of the SLAC1 anion channel** *New Phytol* **218**:1504–1521 <https://doi.org/10.1111/nph.15053>
53. Asai S., Ichikawa T., Nomura H., Kobayashi M., Kamiyoshihara Y., Mori H., Kadota Y., Zipfel C., Jones J.D.G., Yoshioka H (2013) **The variable domain of a plant calcium-dependent protein kinase (CDPK) confers subcellular localization and substrate recognition for NADPH oxidase** *J. Biol. Chem* **288**:14332–14340 <https://doi.org/10.1074/jbc.M112.448910>

54. Valmonte-Cortes G.R., Lilly S.T., Pearson M.N., Higgins C.M., Macdiarmid R.M (2022) **The Potential of Molecular Indicators of Plant Virus Infection: Are Plants Able to Tell Us They Are Infected?** *Plants* **11** <https://doi.org/10.3390/PLANTS11020188/S1>
55. Su C. *et al.* (2023) **Stabilization of membrane topologies by proteinaceous remorin scaffolds** *Nat. Commun* **14**:1–16 <https://doi.org/10.1038/s41467-023-35976-5>
56. Perraki A., Cacas J.L., Crowet J.M., Lins L., Castroviejo M., German-Retana S., Mongrand S., Raffaele S (2012) **Plasma membrane localization of *Solanum tuberosum* Remorin from group 1, homolog 3 is mediated by conformational changes in a novel C-terminal anchor and required for the restriction of potato virus X movement** *Plant Physiol* **160**:624–637 <https://doi.org/10.1104/pp.112.200519>
57. Gronnier J. *et al.* (2017) **Structural basis for plant plasma membrane protein dynamics and organization into functional nanodomains** *Elife* **6** <https://doi.org/10.7554/eLife.26404>
58. Konrad S.S.A., Popp C., Stratil T.F., Jarsch I.K., Thallmair V., Folgmann J., Marín M., Ott T (2014) **S-acylation anchors remorin proteins to the plasma membrane but does not primarily determine their localization in membrane microdomains** *New Phytol* **203**:758–769 <https://doi.org/10.1111/nph.12867>
59. Smokvarska M., Jaillais Y., Martiniere A (2021) **Function of membrane domains in rho-of-plant signaling** *Plant Physiol* **185**:663–681 <https://doi.org/10.1093/PLPHYS/KIAA082>
60. Tran T.M. *et al.* (2020) **The bacterial quorum sensing signal DSF hijacks *Arabidopsis thaliana* sterol biosynthesis to suppress plant innate immunity** *Life Sci. Alliance* **3** <https://doi.org/10.26508/LSA.202000720>
61. Su C., Klein M.-L., Hernández-Reyes C., Batzenschlager M., Ditengou F.A., Lacey B., Keller J., Delaux P.-M., Ott T (2020) **The *Medicago truncatula* DREPP Protein Triggers Microtubule Fragmentation in Membrane Nanodomains during Symbiotic Infections** *Plant Cell* <https://doi.org/10.1105/tpc.19.00777>
62. Grison M.S., Kirk P., Brault M.L., Wu X.N., Schulze W.X., Benitez-Alfonso Y., Immel F., Bayer E.M (2019) **Plasma membrane-associated receptor-like kinases relocate to plasmodesmata in response to osmotic stress** *Plant Physiol* **181**:142–160 <https://doi.org/10.1104/pp.19.00473>
63. Jarsch I.K., Ott T (2011) **Perspectives on Remorin Proteins, Membrane Rafts, and Their Role During Plant–Microbe Interactions** *MPMI* **19** <https://doi.org/10.1094/MPMI>
64. Gui J., Zheng S., Liu C., Shen J., Li J., Li L (2016) **OsREM4.1 Interacts with OsSERK1 to Coordinate the Interlinking between Abscisic Acid and Brassinosteroid Signaling in Rice** *Dev. Cell* **38**:201–213 <https://doi.org/10.1016/j.devcel.2016.06.011>
65. Teixeira R.M., Ferreira M.A., Raimundo G.A.S., Loriato V.A.P., Reis P.A.B., Fontes E.P.B (2019) **Virus perception at the cell surface: revisiting the roles of receptor-like kinases as viral pattern recognition receptors** *Mol. Plant Pathol* **20**:1196–1202 <https://doi.org/10.1111/MPP.12816>
66. Liang P., Stratil T.F., Popp C., Marín M., Folgmann J., Mysore K.S., Wen J., Ott T (2018) **Symbiotic root infections in *Medicago truncatula* require remorin-mediated receptor stabilization in membrane nanodomains** *Proc. Natl. Acad. Sci. U. S. A* **115**:5289–5294 <https://doi.org/10.1073/pnas.1721868115>

67. Gronnier J. *et al.* (2022) **Regulation of immune receptor kinase plasma membrane nanoscale organization by a plant peptide hormone and its receptors** *Elife* **11** <https://doi.org/10.7554/ELIFE.74162>
68. Szymanski W.G., Zauber H., Erban A., Gorka M., Wu X.N., Schulze W.X (2015) **Cytoskeletal components define protein location to membrane microdomains** *Mol. Cell. Proteomics* **14**:2493–2509 <https://doi.org/10.1074/mcp.M114.046904>
69. Stegmann M., Monaghan J., Smakowska-Luzan E., Rovenich H., Lehner A., Holton N., Belkadir Y., Zipfel C (2017) **The receptor kinase FER is a RALF-regulated scaffold controlling plant immune signaling** *Science (80-.)* **355**:287–289 https://doi.org/10.1126/SCIENCE.AAL2541/SUPPL_FILE/STEGMANN_SM_REVISION3.PDF
70. Noack L.C. *et al.* (2022) **A nanodomain-anchored scaffolding complex is required for the function and localization of phosphatidylinositol 4-kinase alpha in plants** *Plant Cell* **34** <https://doi.org/10.1093/PLCELL/KOAB135>
71. Boudsocq M., Droillard M.J., Regad L., Laurière C (2012) **Characterization of Arabidopsis calcium-dependent protein kinases: Activated or not by calcium?** *Biochem. J* **447**:291–299 <https://doi.org/10.1042/BJ20112072>
72. Concordet J.P., Haeussler M (2018) **CRISPOR: intuitive guide selection for CRISPR/Cas9 genome editing experiments and screens** *Nucleic Acids Res* **46**:W242–W245 <https://doi.org/10.1093/NAR/GKY354>
73. Wang Z.P., Xing H.L., Dong L., Zhang H.Y., Han C.Y., Wang X.C., Chen Q.J (2015) **Egg cell-specific promoter-controlled CRISPR/Cas9 efficiently generates homozygous mutants for multiple target genes in Arabidopsis in a single generation** *Genome Biol* **16** <https://doi.org/10.1186/S13059-015-0715-0>
74. Jarsch I.K., Konrad S.S.A., Stratil T.F., Urbanus S.L., Szymanski W., Braun P., Braun K.H., Ott T (2014) **Plasma membranes are Subcompartmentalized into a plethora of coexisting and diverse microdomains in Arabidopsis and Nicotiana benthamiana** *Plant Cell* **26**:1698–1711 <https://doi.org/10.1105/tpc.114.124446>
75. Rohr L, Ehinger A, Rausch L, Glöckner Burmeister N, Meixner AJ, Gronnier J, Harter K, Kemmerling B, zur Oven-Krockhaus S (2024) **OneFlowTraX: a user-friendly software for super-resolution analysis of single-molecule dynamics and nanoscale organization** *Front. Plant Sci* **15** <https://doi.org/10.3389/fpls.2024.1358935>

Editors

Reviewing Editor

Yoselin Benitez-Alfonso

University of Leeds, Leeds, United Kingdom

Senior Editor

Detlef Weigel

Max Planck Institute for Biology Tübingen, Tübingen, Germany

Reviewer #1 (Public review):

Summary:

How plants perceive their environment and signal during growth and development is of fundamental importance for plant biology. Over the last few decades, nano domain organisation of proteins localised within the plasma-membrane has emerged as a way of organising proteins involved in signal pathways. Here, the authors addressed how a non-surface localised signal (viral infection) was resisted by PM localised signalling proteins and the effect of nano domain organisation during this process. This is valuable work as it describes how an intracellular process affects signalling at the PM where most previous work has focused on the other way round, PM signalling effecting downstream responses in the plant. They identify CPK3 as a specific calcium dependent protein kinase which is important for inhibiting viral spread. The authors then go on to show that CPK3 diffusion in the membrane is reduced after viral infection and study the interaction between CPK3 and the remorins, which are a group of scaffold proteins important in nano domain organisation. The authors conclude that there is an interdependence between CPK3 and remorins to control their dynamics during viral infection in plants.

Strengths:

The dissection of which CPK was involved in the viral propagation was masterful and very conclusive. Identifying CPK3 through knockout time course monitoring of viral movement was very convincing. The inclusion of overexpression, constitutively active and point mutation non-functioning lines further added to that.

Weaknesses:

I would like to thank the researchers for including some additional work suggested in the previous round of peer review. However, I still have concerns over this work which are two fold.

(1) Firstly, the imaging described and shown is not sufficient to support the claims made. The PM localisation and its non-PM localised form look similar and with no PM stain or marker construct used to support this. In addition, the quality of lots of the confocal based imaging (including new figure on colocalisation) is simply not sufficient. The images are too noisy and no clear conclusions can be made. The point made previously, the system this data was collected on has an Airyscan detector capable of 120nm resolution and as such NDs can be resolved. The sptPALM data conclusions are nice and fit the narrative. The inclusion of sptPALM movies is useful for the reader and tracks numbers is highly beneficial. But they do not show a high signal to noise ratio compared to other work in the field (see work from Alex Martineire) and the mEOS particles are only just observable over the detector noise in some videos. As such, I worry about the data quality on which the analysis is based on. In addition, in some of the videos the conversion laser seems too high as it is difficult to separate some of the single particles as they emerge which would again, hinder the analysis.

(2) Secondly, remorins are involved in a lot of nano domain controlled processes at the PM. The authors have not conclusively demonstrated that during viral infection the remorin effects seen are solely due to its interaction with CPK3. The sptPALM imaging of REM1.2 in a *cpk3* knockout line goes part way to solve this and the inclusion of CPK3-CA also strengthens the authors claims. But to propose a kiss and go model bearing in mind the differences in diffusion between CPK3 and REM3 and differential changes to diffusion between the two proteins after PIAMV infection without two colour imaging of both proteins at the same time, the claims are much stronger than the evidence. Negative control experiments are required here utilising other PM localised proteins which have no role during viral infection (such as Lti6B).

Overall, I think this work has the potential to be a very strong manuscript but additional evidence supporting interaction claims would significantly strengthen the work and make it exceptional.

<https://doi.org/10.7554/eLife.90309.2.sa2>

Reviewer #3 (Public review):

Summary:

This study examined the role that the activation and plasma membrane localisation of a calcium dependent protein kinase (CPK3) plays in plant defence against viruses. The authors clearly demonstrate that the ability to hamper the cell-to-cell spread of the virus P1AMV is not common to other CPKs which have roles in defence against different types of pathogens, but appears to be specific to CPK3 in Arabidopsis. Further, they show that lateral diffusion of CPK3 in the plasma membrane is reduced upon P1AMV infection, with CPK3 likely present in nano-domains. This stabilisation however, depends on one of its phosphorylation substrates a Remorin scaffold protein REM1-2. However, when REM1-2 lateral diffusion was tracked, it showed an increase in movement in response to P1AMV infection. These contrary responses to P1AMV infection were further demonstrated to be interdependent, which led the authors to propose a model in which activated CPK3 is stabilised in nano-domains in part by its interaction with REM1.2, which it binds and phosphorylates, allowing REM1-2 to diffuse more dynamically within the membrane.

The likely impact of this work is that it will lead to closer examination of the formation of nano-domains in the plasma membrane and dissection of their role in immunity to viruses, as well as further investigation into the specific mechanisms by which CPK3 and REM1-2 inhibit the cell-to-cell spread of viruses, including examination of their roles in cytoskeletal dynamics.

Strengths:

The paper provided compelling evidence about the roles of CPK3 and REM1-2 through a combination of logical reverse genetics experiments and advanced microscopy techniques, particularly in single particle tracking.

Weaknesses:

There is limited discussion or exploration of the role that CPK3 has in cytoskeletal organisation and whether this may play a role in the plant's defence against viral propagation. Further, although the authors show that there is no accumulation of CPK3/Rem1.2 at plasmodesmata, it would be interesting to investigate whether the demonstrated reduction of viral propagation is due to changes in PD permeability.

<https://doi.org/10.7554/eLife.90309.2.sa1>

Author response:

The following is the authors' response to the original reviews.

Public Reviews:

Reviewer #1 (Public Review):

Summary:

How plants perceive their environment and signal during growth and development is of fundamental importance for plant biology. Over the last few decades, nano domain organisation of proteins localised within the plasma-membrane has emerged as a way of organising proteins involved in signal pathways. Here, the authors addressed how a non-surface localised signal (viral infection) was resisted by PM localised signalling proteins and the effect of nano domain organisation during this process. This is valuable work as it describes how an intracellular process affects signalling at the PM where most previous work has focused on the other way round, PM signalling effecting downstream responses in the plant. They identify CPK3 as a specific calcium dependent protein kinase which is important for inhibiting viral spread. The authors then go on to show that CPK3 diffusion in the membrane is reduced after viral infection and study the interaction between CPK3 and the remorins, which are a group of scaffold proteins important in nano domain organisation. The authors conclude that there is an interdependence between CPK3 and remorins to control their dynamics during viral infection in plants.

Strengths:

The dissection of which CPK was involved in the viral propagation was masterful and very conclusive. Identifying CPK3 through knockout time course monitoring of viral movement was very convincing. The inclusion of overexpression, constitutively active and point mutation non functioning lines further added to that.

Weaknesses:

My main concerns with the work are twofold.

(1) Firstly, the imaging described and shown is not sufficient to support the claims made. The PM localisation and its non-PM localised form look similar and with no PM stain or marker construct used to support this. The sptPALM data conclusions are nice and fit the narrative. However, no raw data or movie is shown, only representative tracks. Therefore, the data quality cannot be verified and in addition, the reporting of number of single particle events visualised per experiment is absent, only number of cells imaged is reported. Therefore, it is impossible for the reader to appreciate the number of single molecule behaviours obtained and hence the quality of the data.

(2) Secondly, remorins are involved in a lot of nanodomain controlled processes at the PM. The authors have not conclusively demonstrated that during viral infection the remorin effects seen are solely due to its interaction with CPK3. The sptPALM imaging of REM1.2 in a *cpk3* knockout line goes part way to solve this but more evidence would strengthen it in my opinion. How do we not know that during viral infection the entire PM protein dynamics and organisation are altered? Or that CPK3 and REM are at very distant ends of a signalling cascade. Negative control experiments are required here utilising other PM localised proteins which have no role during viral infection. In addition, if the interaction is specific, the transiently expressed CPK3-CA construct (shown to form nano domains) should be expressed with REM1.2-mEOS to show the alterations in single particle behaviour occur due to specific activations of CPK3 and REM1.2 in the absence of PIAMV viral infection and it is not an artefact of whole PM changes in dynamics during viral infection.

In addition, displaying more information throughout the manuscript (such as raw particle tracking movies and numbers of tracks measured) on the already generated data would strengthen the manuscript further.

Overall, I think this work has the potential to be a very strong manuscript but additional reporting of methods and data are required and additional lines of evidence supporting interaction claims would significantly strengthen the work and make it exceptional.

Reviewer #2 (Public Review):*Summary:*

The paper provides evidence that CPK3 plays a role in plant virus infection, and reports that viral infection is accompanied by changes in the dynamics of CPK3 and REM1.2, the phosphorylation substrate of CPK3, in the plasma membrane. In addition, the dynamics of the two proteins in the PM are shown to be interdependent.

Strengths:

The paper contains novel, important information.

Weaknesses:

The interpretation of some experimental data is not justified, and the proposed model is not fully based on the available data.

Reviewer #3 (Public Review):*Summary:*

This study examined the role that the activation and plasma membrane localisation of a calcium dependent protein kinase (CPK3) plays in plant defence against viruses. The authors clearly demonstrate that the ability to hamper the cell-to-cell spread of the virus P1AMV is not common to other CPKs which have roles in defence against different types of pathogens, but appears to be specific to CPK3 in Arabidopsis. Further they show that lateral diffusion of CPK3 in the plasma membrane is reduced upon P1AMV infection, with CPK3 likely present in nano-domains. This stabilisation however, depends on one of its phosphorylation substrates a Remorin scaffold protein REM1-2. However, when REM1-2 lateral diffusion was tracked, it showed an increase in movement in response to P1AMV infection. These contrary responses to P1AMV infection were further demonstrated to be interdependent, which led the authors to propose a model in which activated CPK3 is stabilised in nano-domains in part by its interaction with REM1.2, which it binds and phosphorylates, allowing REM1-2 to diffuse more dynamically within the membrane.

The likely impact of this work is that it will lead to closer examination of the formation of nano-domains in the plasma membrane and dissection of their role in immunity to viruses, as well as further investigation into the specific mechanisms by which CPK3 and REM1-2 inhibit the cell-to-cell spread of viruses.

Strengths:

The paper provided compelling evidence about the roles of CPK3 and REM1-2 through a combination of logical reverse genetics experiments and advanced microscopy techniques, particularly in single particle tracking.

Weaknesses:

There is a lack of evidence for the downstream pathways, specifically whether the role that CPK3 has in cytoskeletal organisation may play a role in the plant's defence against viral propagation. Also, there is limited discussion about the localisation of the nano-domains and whether there is any overlap with plasmodesmata, which as plant viruses utilise PD to move from cell to cell seems an obvious avenue to investigate.

Recommendations for the authors:

Reviewer #1 (Recommendations For The Authors):

Viral spread work in CPK mutants with time courses is beautiful!

Regarding my public points on my issues with the imaging:

- Figure 2A shows 'PM' localisation of CPK3 and 'non-PM' imaging of CPK3-G2A. The images are near identical both showing cell outlines and cytoplasmic strands. Here a PM marker (such as Lti6B) tagged with a different fluorophore or PM stain should be used in conjunction with surface views (such as in Figure 2C) to show it really is at the PM and the G2A line is not.

Impaired membrane localization of CPK3-G2A is documented in Mehlmer et al., 2010 using microsomal fractionation. Although Figure 2A main purpose is to show correct expression of the constructs in the lines used for PIAMV propagation (Figure 2B), we replaced the images with wider view pictures to be more representative of the subcellular localization of CPK3 and CPK3-G2A.

- Regarding Figure 2C, this is extremely noisy and PM heterogeneity is barely observable over the noise from the system (looking at the edges of surface imaged). You mention low resolution was an issue. I notice from the methods you have taken confocal images on an Zeiss 880 with Airyscan. These images must be confocal but If imaged with Airyscan the PM heterogeneity would be much clearer (see work from John Runions lab).

Indeed, these are tangential views images obtained by Zeiss 880 with Airyscan. Based on tessellation analysis (Figure 2H-J), CPK3 is rather homogeneously distributed and forms ND of around 70nm of diameter. Objects of such size cannot be resolved using pixel reassignment methods such as Airyscan. Note also that AtREM in our study are less heterogeneously distributed than what was described in the literature for StREM1.3.

- Regarding all sptPALM data. At least an example real data image and video is required otherwise the data can't be assessed. The work of Alex Martinieri (sptPALM) or Alex Jonson (TIRF) all show raw data so the reader can appreciate the quality of the data. In addition, number of events (particles tracked) has to be shown in the figure legend, not just number of cells otherwise was one track performed per cell? Or 10,000? Obviously where the N sits in this range gives the reader more or less confidence of the data.

We agree and we added example videos of sptPALM experiments in the supplementary data, we also indicated the number of tracked particles in the figure legends.

- On a slight technical aside, how do you know the cells being imaged for sptPALM with PIAMV are actually infected with the virus? In Fig 2C you use a GFP tagged version but in sptPALM you use none tagged. I think a sentence in methods on this would help clarify.

PIAMV-GFP was used for spt-PALM experiment and cell infection was assessed during PALM experiment. This is now precised in the corresponding figures and methods.

- I also have a concern over some of the representative images showing the same things between different figures. Your clustering data in 3F looks very convincing. However, in Figure 2H the mock and PIAMV-GFP look very similar. How is Figure 3F so different for the same experiment? Especially considering the scale bars are the same for both figures. Same for CPK3-mRFP1.2 in Fig 2C and 3A, the same thing is being imaged, at the same scale (scale bars same size) but the images are extremely different.

Figure 2 data were generated using CPK3 stably expressed in *A. thaliana* while Figure 3 data were obtained upon transient over-expression of CPK3 in *N. benthamiana*. We do not have a clear explanation for such a difference in CPK3 PM behavior, it could lie on a different PM composition or actin organization between those two species, this point is now addressed in the discussion.

- Line 193&194 - you state that the CA CPK3 is reminiscent of the CPK3 upon PIAMV expression. I don't agree, while CPK3CA is less mobile (2D), the MSD shows it is in-between CPK3 and CPK3 + PIAMV. Therefore, can't the opposite also be true? That overall the behaviour of CPK3-CA is reminiscent of WT CPK. I think this needs rewording.

We agree and we reworded that part

- Line 651 - what numerical aperture are you using for the lens during confocal microscopy. This is fundamentally important information directly related to the reproducibility of the work. You report it for the sptPALM.

The numerical aperture is now indicated in the methods.

Regarding my bigger point about specific interactions between CPK3 and remorin during viral infection to strengthen your claim the following need doing. I am not suggesting you do all of these but at least two would significantly enhance the paper.

(1) Image a none related PM protein during viral infection using sptPALM and demonstrate that its behaviour is not altered (such as *Iti6b*). This would show the affects on remorin behaviour are specific to CPK3 and not a whole scale PM alteration in dynamics due to viral infection.

(2) Two colour SPT imaging of CPK3 and REM1.2. You show in absence of proteins (knockouts effect on each other) but your only interaction data is from a kinase assay (where CPK1 and 2 also interact, even though they are not localised at the same place) and colocalisation data (see below). A two colour SPT imaging experiment showing interaction and clustering of CPK3 and REM1.2 with each other and the change in their behaviours when viral infected and simultaneously imaged would address all of my concerns.

- On another note, the co-localisation data (fig 5 sup 4) needs additional analysis. I would expect most PM proteins to show the results you show as the data is very noisy. In order to improve I would zoom in to fill the field of view and then determine correlation and also when one image is rotated 90 degrees (as described in Jarsch et al., plant cell) to enhance this work.

(3) In the absence of viral infection, but presence of CPK3-CA, is sptPALM REM1.2 behaviour in the PM altered, if so then the interaction is specific and changes in remorin dynamics are not due to whole scale PM changes during viral infection and the manuscript substantially strengthened.

(4) Building on from 3), if you have a CPK3 mutated with both CPK3-CA and G2A this would be constitutively active and non-PM localised and as such should not affect Remorin behaviour if your model is true, this would strengthen the case significantly but I appreciate is highly artificial and would need to be done transiently.

Regarding the first point, since the role of PM proteins involved in potexvirus infection is barely assessed, picking a non-related PM protein might be tricky. The data obtained with

mEOS3.2-REM1.2 expressed in cpk3 null-mutant point towards a specific role of CPK3 in PLAMV-induced REM1.2 diffusion and not a general alteration of PM protein behavior.

Regarding the second point, we already reported the *in vivo* interaction between AtCPK3CA and AtREM1.2/AtREM1.3 by BiFC in *N.benthamiana* (Perraki et al 2018) and AtCPK3 was shown to co-IP with AtREM1.2 (Abel et al, 2021). While we agree on the relevance of doing dual color sptPALM with CPK3 and REM1.2, it is so far technically challenging and we would not be able to implement this in a timely manner. For the colocalization, although the whole cell is displayed in the figure, the analysis was performed on ROI to fill the field of analysis.

We agree with the relevance of adding the colocalization analysis of randomized images (mTagBFP2 channel rotated 90 degrees), this is now added to Figure 5 – supplement figure 5.

Finally, for the third and fourth points, spt-PALM analysis of REM1.2 in presence of CPK3-CA and CPK3-CA-G2A was performed (Figure 5 - figure supplement 4). The results suggest a specific role of CPK3-CA in REM1.2 diffusion.

Minor points:

Line 59 - from, I think you mean from.

Line 63 - Reference needed after latter.

Line 68 - Reference required after viral infection.

Line 85 - Propose not proposed.

Line 156 - Allowed us to not allows to.

Line 204 - add we previously 'demonstrated'

Line 622 and 623 - You say lines obtained from Thomas Ott. This is very odd phrasing considering he is an author. I appreciate citing the work producing the lines but maybe reword this

These points were corrected, thank you.

Reviewer #2 (Recommendations For The Authors):

The paper provides evidence that CPK3 plays a role in plant virus infection, and reports that viral infection is accompanied by changes in the dynamics of CPK3 and REM1.2, the phosphorylation substrate of CPK3, in the plasma membrane. In addition, the dynamics of the two proteins in the PM are shown to be interdependent. The paper contains novel, important information that can undoubtedly be published in eLife. However, I have some concerns that should be addressed before it can be accepted for publication.

Major concerns

When the authors say that CPK3 plays a role in viral propagation, it should be clarified what is meant by 'propagation', - replication of the viral genome, its cell-to-cell transport, or long-distance transport via the phloem. By default the readers will tend to assume the former meaning. In my opinion, the term 'propagation' is misleading and should be avoided.

We purposely chose the term “propagation” because it sums replication and cell-to-cell movement. Nevertheless, we previously showed that group 1 StREM1.3 doesn’t alter PVX replication (Raffaele et al., 2009 *The Plant Cell*). In this paper, as we do not investigate the role

of AtREM1.2 or AtCPK3 in the replication of the viral PIAMV genome, we cannot state that these proteins are strictly involved in cell-to-cell movement of the virus.

The authors show that viral infection is associated with decreased diffusion of CPK3 and increased diffusion of REM1.2 in the PM. However, it remains unclear whether these changes are related to partial resistance to viral infection involving CPK3 and REM1.2, or whether they are simply a consequence of viral infection that may lead to altered PM properties and altered dynamics of PM-associated proteins. Therefore, the model presented in Fig. 6 appears to be entirely speculative, as it postulates that changes in CPK3 and REM1.2 dynamics are the cause of suppressed virus 'propagation'. In addition, the model implies that a decrease in CPK3 mobility leads to activation of its kinase activity. This view is not supported by experimental data (see my next comment). The model should be deleted (both as the figure and its description in the Discussion) or substantially reworked so that it finally relies on existing data.

For the first point, the results obtained from the additional experiments proposed by reviewer #1 supports the hypothesis of a direct impact of CPK3 on REM1.2 diffusion (Figure 5 - figure supplement 4).

We agree with the second point and reworked the model to remove the link between CPK3 activation and its increased diffusion.

The statement that 'changes in CPK3 dynamics upon PIAMV infection are linked to its activation' (line 194) is based on a flawed logic, and the conclusion in this section of Results ('changes in CPK3 dynamics upon PIAMV infection are linked to its activation') is incorrect, as it is not supported by experimental data. In fact, the authors show that CPK3 dynamics and clustering upon viral infection is somewhat reminiscent of the behavior of a CPK3 deletion mutant, which is a constitutively active protein kinase. However, this partial similarity cannot be taken as evidence that CPK3 dynamics upon PIAMV infection are related to its activation. Furthermore, the authors emphasize the similarity of the mutant and CPK3 in infected cells without taking into account a drastic difference in their localization (Fig. 3A, middle and right panels) showing that the reduced dynamics or the compared proteins may have different causes. I suggest the removal of the section 'CPK3 activation leads to its confinement in PM ND' from the paper, as the results included in this section are not directly related to other data presented.

The PM lateral organization of PM-bound CPKs in their native or constitutively active form as well as the role of lipid in such phenomenon was never shown before. We believe that this section contains relevant information for the community. We kept the section but reworded it to tamper the correlation made between CPK3 PM organization upon viral infection and its activation.

Line 270 - 'group 1 REMs might play a role in CPK3 domain stabilization upon viral infection'. This is an overstatement. The size of the CPK3-containing NDs may have no correlation with their stability.

We reworded the sentence.

Minor points

Line 204 - we previously that Line 234 and hereafter - "the D" sounds strange. Suggest using "the diffusion coefficient".

This was reworded.

Reviewer #3 (Recommendations For The Authors):

The authors have previously demonstrated that there was an increase in REM1.2 localisation to plasmodesmata under viral challenge. It would be useful to see if there was any co-localisation of REM1.2 and CPK3 with plasmodesmata in response to PLAMV and how this is affected in the mutants. This could be carried out relatively simply using aniline blue.

These experiments were added to the supplementary data of Figure 2 – figure supplement 2. and Figure 4 – figure supplement 4. , no enrichment of CPK3 or REM1.2 at plasmodesmata could be observed upon PLAMV infection.

Fig 3 supplementary figure 2 would be better incorporated into the main body of Figure 3 as this underpins discussion on the involvement of lipids such as sterols in the formation of nanodomains.

We moved Figure 3 – Supplementary figure 2 to the main body of Figure 3.

Minor corrections:

Whilst the paper is generally well written there are a number of grammatical errors:

Line 1 & 2: Title doesn't quite read correctly, suggest a rewording for clarity.

L31: Insert "a" after only

L33: Replace "are playing" with "play"

L34: Begin sentence "Viruses are intracellular pathogens and as such the role..."59: replace "form" with "from"

L63: Insert "was demonstrated" after REM1.2)

L85: Replace "proposed" with "propose"

L86: replace "encouraging to explore" with "which will encourage further exploration of "

L129: replace "we'll focus on" with "we concentrated on"

L131: insert "an" before ATP

L138: change "among" to "amongst"

L156: change "allows to analyse" to "allows the analysis of"

L204: Insert "showed" after previously.

L232: "root seedlings" should this be the roots of seedlings?

L235: insert "to" after "as"

L280: insert "a" after "only"

L281: change " to play" with "as playing": change CA to superscript

L307: Insert "was" after "transcription"

L320: change "display" to "displaying"

L321: change "form" to forms"

L340: "hampering" should come before viral

L365: insert"us' after "allow"

Thank you, these were corrected

<https://doi.org/10.7554/eLife.90309.2.sa0>